

See discussions, stats, and author profiles for this publication at: <https://www.researchgate.net/publication/244990387>

Photo- and Radiation-Chemistry of Halide Anions in Ionic Liquids

ARTICLE *in* THE JOURNAL OF PHYSICAL CHEMISTRY A · JULY 2013

Impact Factor: 2.69 · DOI: 10.1021/jp4042793 · Source: PubMed

CITATIONS

11

READS

30

4 AUTHORS, INCLUDING:



Ilya Shkrob

Argonne National Laboratory

143 PUBLICATIONS 2,163 CITATIONS

[SEE PROFILE](#)



Timothy W Marin

Benedictine University

54 PUBLICATIONS 809 CITATIONS

[SEE PROFILE](#)



James Wishart

Brookhaven National Laboratory

115 PUBLICATIONS 3,638 CITATIONS

[SEE PROFILE](#)

Photo- and Radiation-Chemistry of Halide Anions in Ionic Liquids

Ilya A. Shkrob,*[†] Timothy W. Marin,^{†,‡} R. A. Crowell,*[§] and James F. Wishart*,[§]

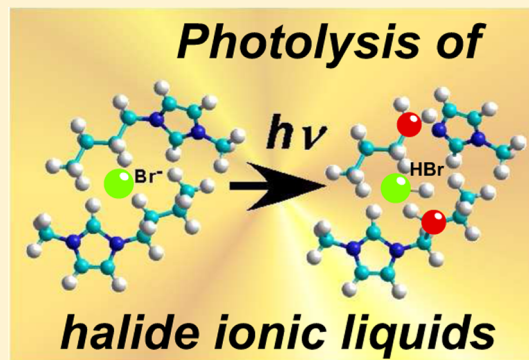
[†]Chemical Sciences and Engineering Division, Argonne National Laboratory, 9700 South Cass Avenue, Argonne, Illinois 60439, United States

[‡]Chemistry Department, Benedictine University, 5700 College Road, Lisle, Illinois 60532, United States

[§]Chemistry Department, Brookhaven National Laboratory, Upton, New York 11973-5000, United States

S Supporting Information

ABSTRACT: One- and two-photon excitation of halide anions (X^-) in polar molecular solvents results in electron detachment from the dissociative charge-transfer-to-solvent state; this reaction yields a solvated halide atom and a solvated electron. How do such photoreactions proceed in ionic liquid (IL) solvents? Matrix isolation electron paramagnetic resonance (EPR) spectroscopy has been used to answer this question for photoreactions of bromide in aliphatic (1-butyl-1-methylpyrrolidinium) and aromatic (1-alkyl-3-methyl-imidazolium) ionic liquids. In both classes of ILs, the photoreaction (both 1- and 2-photon) yields bromine atoms that promptly abstract hydrogen from the alkyl chains of the IL cation; only in concentrated bromide solutions (containing >5–10 mol % bromide) does $\text{Br}_2\cdot^{\bullet}$ formation compete with this reaction. In two-photon excitation, the 2-imidazolyl radical generated via the charge transfer promptly eliminates the alkyl arm. These photolytic reactions can be contrasted with radiolysis of the same ILs, in which large yield of BrA^{\bullet} radicals was observed (where A^- is a matrix anion), suggesting that solvated Br^{\bullet} atoms do not occur in the ILs, as such a species would form three-electron $\sigma^2\sigma^{*1}$ bonds with anions present in the IL. It is suggested that chlorine and bromine atoms abstract hydrogen faster than they form such radicals, even at cryogenic temperatures, whereas iodine mainly forms such bound radicals. These XA^{\bullet} radicals convert to $\text{X}_2\cdot^{\bullet}$ radicals in a reaction with the parent halide anion. Ramifications of these observations for photodegradation of ionic liquids are discussed.



1. INTRODUCTION

In polar molecular liquids with no electron affinity (including water, alcohols, and acetonitrile), one- and two-photon excitation of halide (X^-) and pseudohalide anions results in the formation of the charge-transfer-to-solvent state (CTTS) of these anions^{1–8} that within 100 fs^{1,2a} ejects the excess electron into the solvent (see ref 1 for review).



This photoejected electron thermalizes and localizes^{1–6} near the oxidized anion (that relaxes in <300 fs).² In aqueous solution, the interaction between the geminate partners is weak (a few kT),^{1,2,6,8} and thermally activated dissociation of (X^{\bullet} , $\text{e}_{\text{solv}}^{-\bullet}$) pairs occurs in a few tens of picoseconds. The quantum yield for the initial charge separation is high (0.1–1), approaching unity for halide anions;^{1,2,6,7} and the yield of free solvated electrons is lower, typically 0.1–0.5 (as such pairs recombine back by the diffusion of the geminate partners).⁶ The nature of the weak interactions responsible for the cage effect remains uncertain,¹ but the one-electron soft pseudopotential model of Staib and Borgis did produce the shallow mean force potentials for aqueous chloride.⁸ The caveat is that halide atoms form a three-electron $\sigma^2\sigma^{*1}$ bond with the oxygen atom in one of the water molecules in the first solvation shell,^{9–12}

whereas current models do not explicitly consider such covalent interactions. In this bound molecule, the O–H dipoles are oriented in a fashion^{10–12} favoring electron solvation in the adjoining cavity,⁸ so it may contribute to “gluing” the solvated electron and its partner, possibly accounting for the formation of metastable solvent-separated (X^{\bullet} , $\text{e}_{\text{solv}}^{-\bullet}$) pairs. Ultrafast laser spectroscopy^{1–6} indicates that the photoejected electron is fully solvated within <1 ps of the photoexcitation, suggesting that the local environment around the electron in the geminate (X^{\bullet} , $\text{e}_{\text{solv}}^{-\bullet}$) pair is virtually the same as in the bulk solvent. On a longer time scale, the X^{\bullet} atom (that is, the photooxidized halide anion) reacts with X^- anions in solution



yielding the $\text{X}_2\cdot^{\bullet}$ radical, which is another example of a $\sigma^2\sigma^{*1}$ bound radical. Secondary reactions of the solvated electrons, X^{\bullet} atoms, and $\text{X}_2\cdot^{\bullet}$ radicals generate X_2 and X_3^- species,^{9,13} and the resulting chemistry is quite involved, with multiple cross-reactions unfolding on the nanosecond and microsecond time scales.⁹

Received: April 30, 2013

Revised: June 10, 2013

Published: June 21, 2013



While the general outline of this halide photochemistry in molecular solvents is well understood, photoreactions occurring in room-temperature ionic liquids (ILs)¹⁴ have only begun to be studied recently. ILs are organic salts with low melting points.^{14–16} Over the last 15 years, there has been an explosion of interest in such liquids and their applications, largely driven by their unique properties: combinatorial versatility, low flammability and volatility, electric conductance, and superior solvation properties. ILs have been suggested as replacements of molecular solvents, diluents, and electrolytes in numerous applications:¹⁴ in preparative organic synthesis, batteries, photovoltaics, and nuclear used fuel treatment,^{15,16} to name just a few areas. ILs based on halide and pseudohalide (e.g., imide) anions are among the largest classes of practically important ILs,^{14,15} hence our interest in this class of compounds. Some of these applications involve exposure of the ILs to voltage overpotential, light, and radiation that induce redox reactions involving the constituent ions, which cause gradual degradation of the ILs.^{15,16} While radiation chemistry of the ILs has been extensively studied (including our own work),^{15,17–23} their photochemistry remains less understood.

In the following, we will make the distinction between the ILs that are composed of aromatic cations (C^+), such as 1-alkyl-3-methyl imidazolium ($C_n\text{mim}^+$, which are the progenitors of most practically important ILs), and aliphatic cations that include tetraalkyl (N_{abcd}^+) ammonium and phosphonium salts and their cyclical analogues (such as pyrrolidinium, guanidinium, morpholinium, etc.). See Scheme 1S in the Supporting Information for the structures of these ions.

The ultraviolet (UV) photoexcitation of ILs ($C^+\text{A}^-$) can potentially involve both of the constituent ions. However, for UVB photoexcitation, the photoabsorption would be expected to involve mainly the halide anion, and the photoreaction was expected to proceed like the photo-CTTS reaction described above.^{24–26} Katoh et al.²⁷ studied iodide in an aliphatic IL, trimethylbutylammonium bis(triflimide), and observed a well-defined CTTS band that was centered at 225 nm and extended down to 250 nm. One-photon excitation of this band yields the characteristic 1.1 μm absorption of the solvated electron $e_{\text{solv}}^{-\bullet}$ that was similar to the one observed in pulse radiolysis of neat IL solvent.¹⁵ At later delay time, $I_2^{-\bullet}$ is gradually formed via reaction 2.²⁷ The quantum yield for the free $e_{\text{solv}}^{-\bullet}$ was estimated to be 0.34, which is comparable to that observed in other polar liquids; e.g., ref 6. Addition of $C_4\text{mim}^+$ resulted in rapid scavenging of $e_{\text{solv}}^{-\bullet}$ through electron attachment, and the extrapolated lifetime of the excess electron in neat $C_4\text{mim}$ NTF₂ was estimated to be ~ 350 ps, which is likely to be grossly overestimated.²⁷ Unterreiner and co-workers^{24–26} did observe short-lived (<10 ps) transient absorbance in the near-infrared (1.2–1.5 μm) following 257 nm laser photoexcitation of $C_n\text{mim}$ X liquids ($n = 6, 10$ and $X = \text{Cl}, \text{I}$) that was attributed to a cavity electron (before it attaches to the aromatic cation).^{24–29} An alternative interpretation²⁴ is that this absorbance may result from a $\sigma \leftarrow \sigma^*$ transition in the $C_2^{+\bullet}$ dimer cation (Scheme 2S, Supporting Information), as discussed below.^{17,18}

The analogy with photo-CTTS reaction 1 becomes less obvious for aromatic ILs (that have accessible π -systems) and also for halide anions other than iodide in aliphatic ILs, as the excitation energy increases, making other reaction channels possible. This analogy becomes particularly strained in concentrated IL solutions, as the solvent itself consists of halide anions.²⁴ That the photoexcitation of X^- anion in such

photosystems mainly results in charge separation has not been demonstrated. It is also unclear that charge separation in aromatic ILs (given the ease of cation reduction) involves two distinct stages (electron photoejection reaction 1 followed by electron attachment, reactions 3 and 4)

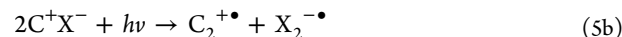


as opposed to direct charge transfer



as has been observed by Chandrasekhar and Unterreiner in their recent review.²⁴

The excess electrons (analogous to *F*-centers in ionic crystals) stabilized by the Coulomb interaction with several IL cations have been observed in many aliphatic ILs in pulse radiolysis–transient photoabsorption (TA) experiments,¹⁵ but their presence (even as short-lived metastable species) in aromatic ILs has been the subject of controversy,^{17,19,24,27–29} as these aromatic cations have large electron affinities. EPR studies^{17,19} indicate that imidazolium cations eventually accept an electron to yield 2-imidazolyl radicals (C^\bullet); in some ILs, these σ -radicals further react to form a $\sigma^2\sigma^{*1}$ C–C bond with the parent cation, thereby yielding a dimer radical cation, $C_2^{+\bullet}$. See Scheme 2S in the Supporting Information for the structural formulas of these radicals. For pyridinium cations,³⁰ stacked π -dimers have been identified as trapped-electron centers: two of such cations assume an antiparallel sandwich arrangement to share the excess electron as a $C_2^{+\bullet}$ species. Radiolysis of neat halide ILs also results in the formation of $X_2^{-\bullet}$ radicals that are readily observed through their $\sigma \leftarrow \sigma^*$ optical transition^{31–33} and by EPR.¹⁸ Given the high concentration of parent X^- anions in such ILs, one can expect that the released X^\bullet either promptly yields $X_2^{-\bullet}$ ^{13,24} (which makes the overall reaction more exothermic) or the charge transfer is concerted with the $X_2^{-\bullet}$ radical formation.¹⁷



Regardless of the exact mechanism, the corresponding photoreactions rapidly yield a geminate pair of C^\bullet (or $C_2^{+\bullet}$) and X^\bullet (or $X_2^{-\bullet}$) radicals. The pair can recombine back to generate the parent cations, C^+ and X^- , or (conceivably) C_2 and X_2 species (section 4.2).^{17,20} Rapid dimerization in the geminate partners, reaction 5b, can assist in overcoming back recombination in close pairs. That the Cl^\bullet atom is a distinctive reaction intermediate even at high halide concentration is suggested by our observation¹⁸ that in radiolysis of chloride ILs consisting of aromatic or aliphatic anions with alkyl arms no $\text{Cl}_2^{-\bullet}$ radical is observed by EPR, suggesting that the released Cl^\bullet atom promptly abstracts H from the aliphatic arms (forming the corresponding $\text{C}(-\text{H})^{+\bullet}$ radical). Even in neat chloride ILs, this H-abstraction reaction occurs more rapidly than reaction 2.¹⁸ Since in the gas phase, the H–Cl bond is much stronger than H–Br and H–I bonds (4.43 eV vs 3.76 and 3.06 eV, respectively, which should be compared with 4.13 eV for a typical C–H bond in the alkyl arm, see Table 1S in the Supporting Information), this H abstraction does not fully inhibit $X_2^{-\bullet}$ radical formation in halide ILs other than chloride. In chloride ILs consisting of aromatic cations with benzyl arms,³⁰ this H-abstraction is slower than reaction 2, and the corresponding trapped-electron centers and the $\text{Cl}_2^{-\bullet}$ radicals have equal yield.

In this article, we use EPR spectroscopy to address the photochemistry of bromide ILs, seeking to directly observe the postulated reaction intermediates. Bromide was chosen as it is the only halide anion for which these intermediates can be observed by EPR (chloride atoms are too reactive and iodine species exhibit rapid spin relaxation). Our results indicate that the chemistry significantly differs from reaction 1.

In particular, we demonstrate that radiolytic oxidation of bromide in dilute IL solutions ($C^+ A^-$) yields $\sigma^2\sigma^{*1}$ bound BrA^- radical anions, where A^- is the solvent (matrix) anion; there are, actually, no trapped halide atoms in ILs, as the interactions with anions are much stronger than interactions with neutral molecules. Furthermore, neither one-photon nor two-photon excitation of bromide containing IL solutions yields even these BrA^- radicals; instead, the photoreleased Br^\bullet atom promptly abstracted H from the aliphatic arms of a cation (like the chlorine atoms in radiolytic experiments). Only when the mole fraction of Br^- is high (>0.1) do some of these Br^\bullet atoms decay in reaction 2. Another unexpected result is that instead of mild photoinduced charge transfer reactions 5a and 5b (as visualized above), two-photon excitation causes elimination of alkyl arms from the cation.

To save space, supporting schemes, tables, and figures, and a list of abbreviations and reactions are placed in the Supporting Information. When referenced in the text, these materials have the designator "S", as in Scheme 1S.

2. EXPERIMENTAL AND COMPUTATIONAL METHODS

Unless specified otherwise, ILs (Scheme 1S) and reagents were obtained from Aldrich and used without further purification. Optical quality 1-butyl-1-methylpyrrolidinium bis(triflimide) ($P_{14}NTf_2$) was obtained from Iolitec. In the following, tetraalkylammonium cations are designated as N_{abcd}^+ , where the indices indicate the carbon numbers in *n*-alkyl arms, and 1-(*n*-alkyl)-3-methylimidazolium cations are referred to as C_n mim⁺. The anions in the IL solvents were pseudohalides, bis(triflimide) (NTf_2^-), and dicyanamide (DCA^- , $N(CN)_2^-$); triflate (TfO^-) was used to provide a reference system in section 3.2 (Scheme 1S). Ionic liquids and their solutions were dried in a vacuum oven for 3–4 h before the glass sample tubes were flame-sealed, and contained <100 ppm of water or protic impurities by proton magnetic resonance. In the following, bromide doped solid samples are designated as, for example, C_n mim NTf₂:Br, meaning a frozen solution of C_n mim NTf₂ containing 0.1–10 mol % C_n mim Br.

For EPR spectroscopic measurements, solid or liquid samples placed in o.d. 4 mm Suprasil tubes were frozen by rapid immersion in liquid N₂ and subsequently irradiated at 77 K. In radiolysis experiments, we used 2.5 MeV electrons and irradiated samples to 3 kGy (1 Gy = 1 J/kg) over 1 min. For photolysis, we used either 266 nm (<1 mJ) and 355 nm (<35 mJ) light pulses (6 ns fwhm, 6 mm 1/e diameter, 10 Hz repetition rate) from a Nd:YAG laser (Quantel) or filtered output from a 60 W xenon arc lamp. The samples were immersed in liquid nitrogen during the irradiation and then quickly transferred to the EPR resonator for spectroscopic measurements.

The radicals were observed using a 9.44 GHz Bruker ESP300E spectrometer, with the sample tube placed in a flow helium cryostat (Oxford Instruments CF935) that allowed cycling of the temperature between 10 and 250 K. The magnetic field B and the hyperfine coupling constants (hfccs) are given in the units of Gauss ($1 G = 10^{-4} T$). If not stated

otherwise, the first-derivative EPR spectra were obtained at 50 K using 100 kHz field modulation. The modulation amplitude was 2 G for organic radicals (400 G field sweep) and 8–10 G for bromine radicals (2–3 kG field sweep). The radiation-induced EPR signal from the E'_γ center and trapped H^\bullet atoms in the Suprasil sample tubes (that frequently overlapped with the resonance lines) is whited out in the EPR spectra given in the figures. It is also noteworthy that due to the large span of the EPR spectra, broad features from paramagnetic impurities in the resonator partially overlapped the (much narrower) resonance lines from bromine related radicals.

The calculations of the gas-phase energetics (Tables 1S to 5S) and hfccs (Tables 6S and 7S) were carried out using a density functional theory (DFT) method with the B3LYP functional³⁴ and 6-31+G(d,p) basis set from Gaussian03.³⁵ In the following, *a* denotes the isotropic hfcc and *B* the anisotropic (traceless) part of the hfc tensor *A* with the principal axes (*a,b,c*) (unless they were aligned with the g-tensor). Powder EPR spectra were simulated using standard first-order perturbation theory. The quadrupole interaction with ^{79,81}Br nuclei was neglected. For Br-related radicals, only longitudinal (\parallel) components of the axially symmetrical *A* and *g* tensors can be attributed, due to the congested and complicated EPR spectra. Bromine has two naturally abundant spin-3/2 isotopes, ⁷⁹Br and ⁸¹Br, with abundances of 50.7% and 49.3%, and hfccs for the latter are 7.9% greater; this further complicates the EPR spectra.

3. RESULTS

3.1. Radiolysis and Photolysis of Neat C_n mim Br. In ref 18, we studied radicals generated in radiolysis of frozen C_6 mim Br. At low temperature (<120 K), two radical species gave the largest contributions to the observed EPR spectrum: the 2-imidazolyl radical (C^\bullet ; see Scheme 2S) and Br_2^- . There was no evidence for the $C_2^{+•}$ radical formation in this IL; the $C_2^{+•}$ radical was observed only in radiolysis of C_n mim NTf₂.^{18,19} Some C_n mim⁺ cations also become oxidized in the energetic radiolytic events, and the corresponding dication $C^{2+•}$ promptly deprotonates to yield $C(-H)^{+•}$ radicals,^{19,21,23} as shown in Scheme 2S, whose resonance lines superimpose on the resonance line of the $C^\bullet/C_2^{+•}$ radicals. Warming of the irradiated sample above 170 K facilitates charge recombination and causes the appearance of a protonated form of 2-imidazolyl, that is the $CH^{+•}$ radical.^{18,19} The EPR spectra of irradiated polycrystalline C_2 mim Br and C_4 mim Br (that were used to prepare solutions studied below) obtained at 50 K were qualitatively similar to that of C_6 mim Br in ref 18 (Figure 1S). Well-resolved lines of Br_2^- were observed, with $g_\parallel \approx 1.973$ and $A_\parallel(^{81}\text{Br}) \approx 457$ G, which are similar to the parameters for Br_2^- radicals (V_K centers) in inorganic halide crystals (Table 8S).

Even protracted photolysis of these crystalline C_n mim Br solids using 266 nm laser light and UV light from a lamp at 77 K did not result in a sufficient radical yield to be measured by EPR (which is one of the most sensitive spectroscopies, with typical detection limits $<10^{15} \text{ cm}^{-3}$). In contrast, 355 nm laser excitation of C_2 mim Br (Figure 2S) and C_4 mim Br yielded EPR spectra like the one shown in Figure 1S. Resonance lines from Br_2^- were observed once again (the $M(2Br) = +1$ line being the most prominent), indicating the occurrence of charge separation (Figure 2Sb). The greatest surprise is the central part of the EPR spectrum shown separately in Figures 1 and 2Sa. The main contribution to this spectrum is provided by an alkyl radical whose resonance lines (with the characteristic 25 G

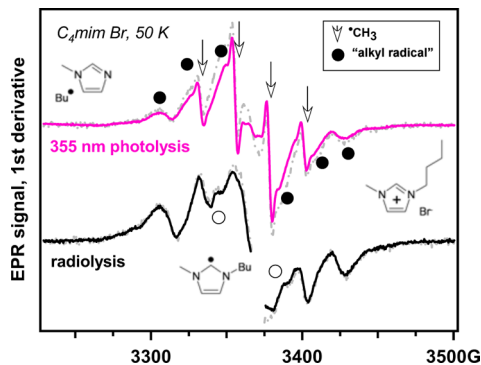


Figure 1. First-derivative EPR spectra of $C_4\text{mim Br}$ (quenched melt) photoirradiated by 355 nm laser light ($0.12 \text{ J}/\text{cm}^2$) at 77 K (50 K, 2 mW, and 2 G modulation). The EPR spectrum obtained in 2.5 MeV electron radiolysis of the same sample is dominated by the contributions from C^\bullet radicals (open circles) and $C(-H)^{+\bullet}$ radicals (filled circles). In the EPR spectra of laser-irradiated samples, the doublet of the 2-imidazolyl radical is not observed, and the EPR spectrum is a superposition of resonance lines from R^\bullet , $C(-H)^{+\bullet}$, and methyl radicals.

splitting pattern) are indicated with filled circles in the plot. Overlapped with this EPR spectrum are four narrow resonance lines from the methyl radical. Such products can be generated through dissociative electron attachment (DEA) to the parent cation that causes scission of the C–N bonds, yielding a terminal alkyl radical and a residual base, with the preference for the elimination of a longer arm.

In section 3.3, it will be demonstrated that 355 nm photon excitation is biphotonic (which can already be inferred from the fact that $C_n\text{mim Br}$ does not absorb 355 nm light), so there is sufficient excess energy to access excited states that undergo charge transfer in concert with the dissociation of the 2-imidazolyl radical. DFT calculations presented in ref 19 indicated low reaction barriers (<200 meV) for alkyl arm elimination in the 2-imidazolyl radical, and our recent studies³⁰ indicate that the benzyl radical is readily eliminated from reduced 1-benzyl-3-methylimidazolium and its 1,2,4-triazoalium analogue in radiolysis. Therefore, even small excess energy in the residual 2-imidazolyl radical can cause its dissociation. In radiolysis, the excess electron ejected from the bromide anion fully thermalizes before the attachment to the cation, yielding stable 2-imidazolyl radicals. In contrast, biphotonic excitation yields electronically or vibronically excited 2-imidazolyl radicals that promptly dissociate.

Below, we will also present evidence that some of these alkyl radicals are, actually, $C(-H)^{+\bullet}$ radicals (that have similar EPR spectra) that are generated in reactions of the photoreleased Br^\bullet atoms that abstract hydrogen from the parent cation. According to our DFT calculations (Table 1S), the gas-phase C–H bond dissociation energies for methyl and ethyl arms of $C_2\text{mim}^+$ are 4.91 eV (Me), 3.93 eV (α), and 4.38 eV (β), respectively. The energy of the H–Br bond in gas-phase HBr is 4.03 eV (by DFT calculation, Table 2S) or 3.87 eV (by experiment). As seen from these energetics (that do not include solvent effects), even a small excess energy in the bromine atom can facilitate abstraction of α -hydrogen in the long arm of the cation. This reaction can be preferred to the addition of the bromine atom to the cation at carbon-2, which is only slightly exothermic (by 0.375 eV, according to our DFT calculation, Table 1S). We have searched but did not find an EPR signature

of such Br atom adducts either in neat bromide ILs or their solutions.

3.2. Radiolysis of Bromide in IL Solutions. What happens when the bromide anion is oxidized in dilute IL solutions? Simple mindedly, one can expect the formation of a trapped bromine atom. As the diffusion of this atom is inhibited in a low temperature solid, in a dilute IL solution, only a small fraction of these trapped atoms can react with dispersed Br^- anions to form $\text{Br}_2^{-\bullet}$ in reaction 2. As the matrix warms, the diffusion of Br^\bullet atoms is thermally activated, reaction 2 occurs, and the $\text{Br}_2^{-\bullet}$ species becomes predominant.

The problem with this scenario (which is fully analogous to the outcome of reaction 1 occurring in molecular solvents) is that it is not clear whether such trapped Br^\bullet atoms can even exist in ILs. Indeed, the Br^\bullet atom is known to form bound $\text{BrX}^{-\bullet}$ radicals with other halide (Cl^- , Br^-) and pseudohalide (SCN^- , OH^-) anions.^{13,31–33} Numerous $\sigma^2\sigma^{*1}$ complexes of Cl^\bullet with neutral molecules (water, NH_3 , PMe_3 , and pyridine) and anions (X^- , OH^- , and succinimide) are known (see Table 9S).¹⁰ In these complexes, a significant fraction of the unpaired electron density is shared by the partner, resulting in superhyperfine structure arising from electron coupling to the magnetic nuclei bound to the halide.

For bromine atom, direct EPR observations have been scarce, see Table 10S, precisely due to the propensity of Br^\bullet to form weak bond complexes with the matrix. The study that is most relevant to the present one is by Muto and Kispert,³⁶ who studied irradiated single crystals of *N*-bromosuccinimide. Succinimide is a pseudohalide anion resembling DCA^- and NTf_2^- . X-ray irradiation of *N*-bromosuccinimide yields two radicals, I and II. These radicals have similar A tensors for ^{81}Br and ^{79}Br ; the main difference being that radical I exhibits significant hfcc on ^{14}N nuclei with $a \approx 48 \text{ G}$, while radical II was not coupled to nitrogen-14. Muto and Kispert³⁶ suggest that radical I is $\text{BrA}^{-\bullet}$ (where A^- is succinimide) resulting from electron attachment to the parent molecule



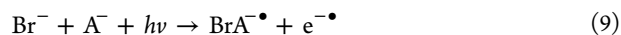
whereas radical II is fully dissociated radical I originating in DEA.

We observe that the same $\text{BrA}^{-\bullet}$ species can also be generated through reactions taking place in ionic liquids, those being



Reaction 2 is but a particular example of reaction 7. In section 4.1, we demonstrate that both reactions 7 and 8 are strongly exergonic in the gas phase.

These general considerations and energetics given in Table 4S suggest that isolated Br^\bullet atom is unlikely to persist in ILs, as it should form a $\text{BrA}^{-\bullet}$ radical, pairing with the matrix anions via reaction 7. So, instead of reaction 1, the actual photo-reaction is likely to be



followed by



Unlike UV photolysis (that involves selective excitation of the bromide), radiolysis excites and ionizes all of the ions present in the IL system, so in dilute IL solutions reactions 1

and 7 become unlikely, and the most likely chemical path to bromide oxidation is reaction 8. Reaction 10 occurs provided that the Br–Br bond in $\text{Br}_2\cdot^\bullet$ radical is stronger than the Br–A bond in the BrA^\bullet radical (see section 4.1). This can be expected for most anions other than iodide and thiocyanate. The formation of BrSCN^\bullet radicals in the reaction of $\text{Br}_2\cdot^\bullet$ with SCN⁻ in radiolysis of N₁₄₄₄ SCN:Br was observed in pulse radiolysis–transient absorption experiments of Grodkowski et al.^{32,33}

Figure 2 shows the EPR spectra of radicals observed in irradiated C₂mim DCA:Br. While there is almost no evolution

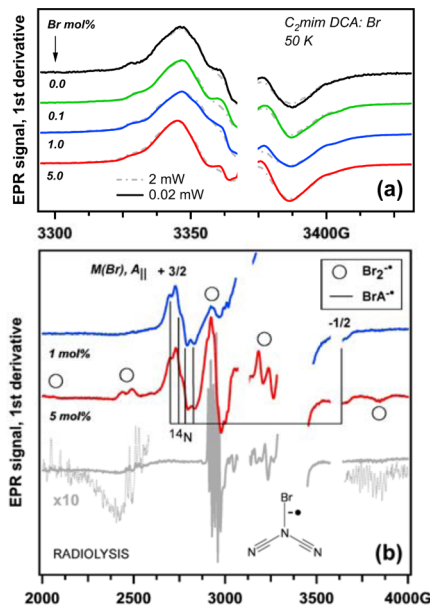


Figure 2. (a) Normalized first-derivative EPR spectra of C₂mim DCA:Br (frozen solution) irradiated by 2.5 MeV electrons at 77 K (observed at 50 K and 2 G modulation). Solid lines for 0.02 mW; dashed lines for 2 mW. There is little evolution of these spectra with varying bromide concentration, and the main contribution is from the C• radical. The mole fraction of bromide is indicated in the plot. (b) Wide-sweep EPR spectra (8 G modulation) observed in 1 and 5 mol % bromide solutions. For comparison, the EPR spectrum of $\text{Br}_2\cdot^\bullet$ is shown at the bottom (the corresponding resonance lines are indicated with open circles). Discernible resonance lines from the BrA^\bullet radical are indicated in the plot. Note the superhyperfine structure in the $M(\text{Br}) = +3/2$ line due to coupling to the unique ¹⁴N nucleus (see the inset).

of EPR spectra of organic radicals (which is mainly from the 2-imidazolyl radical, see in Figure 2a), there is significant evolution of the EPR spectra from bromine related radicals shown in Figure 2b. As the mole fraction of bromide decreases from 5 mol % to 1 mol %, the resonance lines from $\text{Br}_2\cdot^\bullet$ become weaker and new lines appear. These resonance lines have strong resemblance to Br• atom observed by Griscom in irradiated bromide-doped potassium borate glass.³⁷ Griscom reasoned that for this species $A_\perp \approx A_{\parallel}/2$ (for ^{79,81}Br) and obtained $g_\perp \approx 2.26$, $g_\parallel \approx 1.909$, and $A_{\parallel}(\text{Br}) \approx 485$ G (Table 10S). Making the same assumption, we estimated $g_\perp \approx 2.18$, $g_\parallel \approx 1.984$, and $A_{\parallel}(\text{Br}) \approx 452$ G. As seen from Figure 2b, there is superhyperfine structure in the $M(\text{Br}) = +3/2$ line resulting from hyperfine coupling to a single nitrogen-14 with $A_{\parallel}(\text{N}^{14}) \approx 48$ G, which conclusively proves that the suspected Br• atom is, in fact, a BrA^\bullet radical (section 4.1).

The same spectral transformations were observed for C₄mim DCA:Br (Figure 3S). When the irradiated sample containing 1 mol % and 10 mol % bromide was warmed over 125 K (Figures 4S and 3, respectively), the resonance lines from the BrA^\bullet

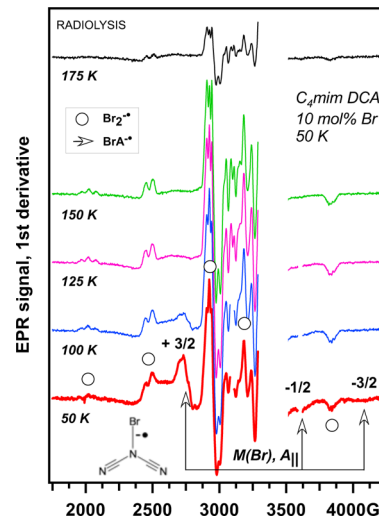


Figure 3. Evolution of EPR spectra from radiolyzed C₄mim DCA containing 10 mol % bromide upon slow warming of the sample. As the diffusion of BrA^\bullet radical becomes activated above 100–125 K, this species reacts with the bromide and converts to $\text{Br}_2\cdot^\bullet$. Symbols have the same meaning as in Figure 2.

radical disappeared, and only the $\text{Br}_2\cdot^\bullet$ radical was observed. This behavior agrees with the occurrence of thermally activated reaction 10.

We next examined C₄mim TfO:Br (Figure 4). Changes in the EPR spectra of organic radicals were again small (Figure 4a), whereas variations in the EPR spectra of the Br-related radicals shown in Figure 4b were significant. Without bromide, weak resonance lines of $\cdot\text{CF}_3$ and $\cdot\text{CF}_2\text{SO}_3^-$ radicals were observed in the background.^{18,21} In 1 mol % and 10 mol % bromide solutions, these resonance lines were overwhelmed by the lines from BrA^\bullet and $\text{Br}_2\cdot^\bullet$ radicals (Figure 4b). No superhyperfine structure was discernible in the $M(\text{Br}) = +3/2$ line of the majority variant of the BrA^\bullet radical (radical I). This indicates that bromine is coupled to oxygen-16, which is not magnetic (see the insets in Figure 4b). A closer inspection of Figure 4b indicates the presence of another (minority) variant of the center (radical II) that has a 27% larger $A_{\parallel}(\text{Br})$ constant, suggesting that the bromine atom has two modes of interaction with a triflate anion. The $M(\text{Br}) = +3/2$ resonance line in radical II is a doublet, indicating that in radical II, the unpaired electron is coupled to fluorine-19 ($A_{\parallel}(\text{F}) \approx 41.5$ G), which is a spin-1/2 nucleus (see the inset in Figure 4b).

When C_nmim NTf₂:Br solutions were examined, the evolution of the EPR spectrum from organic radicals was observed (Figure 5a). In C_nmim NTf₂, the trapped-electron center is C₂⁺, whereas in C_nmim Br, it is C•; in ref 18, we suggested that the likely cause is lower energy for dissociation of the corresponding C⁺A⁻ pairs required for the formation of C₂⁺.^{17,18} Gradual dilution of C_nmim Br with C_nmim NTf₂ transforms the EPR spectrum from the doublet of C• to the singlet of C₂⁺ (Figure 5a). Concomitant with these transformations is the gradual disappearance of $\text{Br}_2\cdot^\bullet$ from the EPR spectrum and the appearance of the resonance lines from the BrA^\bullet radical, which exists in two variants (Figure 5b). Radical

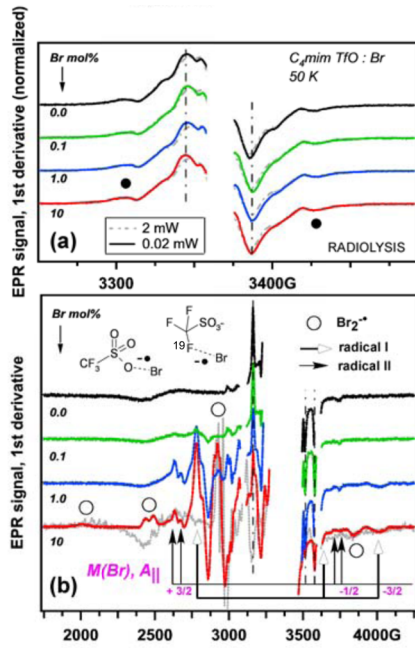


Figure 4. Same as that in Figure 2, for C_n mim TfO containing bromide. In panel a, filled circles indicate the resonance lines of $C(-H)^{+•}$ radicals. In panel b, resonance lines from the majority and minority variants of the $BrA^{-•}$ radical (I and II, respectively) are indicated as shown in the inset (to the left and to the right, respectively). The suggested chemical structures for these radicals are sketched in the inset. Vertical dash-dot lines indicate the positions of resonance lines from $^{*}CF_3$ and $^{*}CF_2SO_3^-$ radicals generated in radiolytically induced decomposition of the triflate anion.

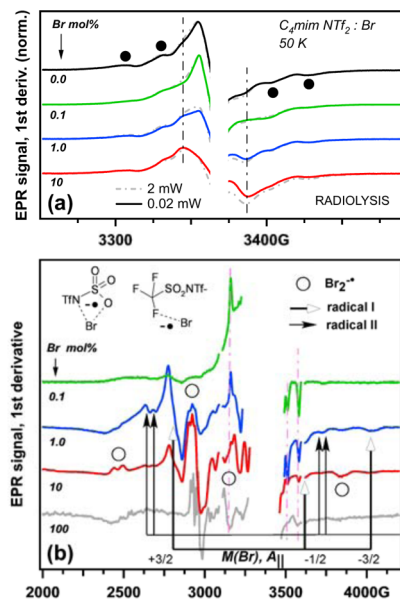


Figure 5. Like Figure 4, for C_4 mim NTf₂:Br. In panel b, 100 mol % Br corresponds to neat C_4 mim Br.

I has an almost featureless $M(Br) = +3/2$ line ($A_{||}(^{81}Br) \approx 409$ G), whereas radical II has a greater hfcc (by ~33%) and the same resonance line is a doublet indicative of ^{19}F splitting ($a \approx 46$ G). On the basis of the analogy with triflate (see above), we suggest that radical I is bromine coupled to N- or O-atoms in the bistriflimide anion, whereas radical II is the bromine coupled to the trifluoromethyl group of the same anion (see the

inset in Figure 5b). Upon warming of the 1 mol % sample from 50 to 125 K (Figure 5S), both radical I and radical II disappear, with the more weakly bound radical II disappearing before radical I, and only the $Br_2^{-•}$ radical persists to 175 K. This can be used to isolate the spectrum of radical I, as shown in Figure 6. It is seen from Figure 5S that the decay of radical I at 150 K

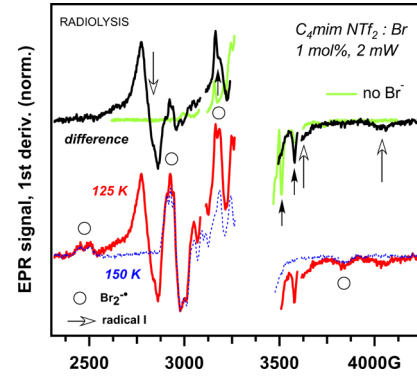


Figure 6. Isolating the spectrum of radical I (open arrows) from the raw data shown in Figure 5S in the Supporting Information. Radical II fully decayed at 125 K, while radical I persisted; however, the corresponding spectrum contains additional resonance lines from $Br_2^{-•}$ radical (open circles). The latter can be subtracted at 150 K. (At this temperature, there is complete conversion of radical I to $Br_2^{-•}$.) The difference spectrum is shown at the top and compared to the EPR spectrum observed in radiolyzed C_4 mim NTf₂ (light green line). The lines of $^{*}CF_3$ and $^{*}CF_2SO_2NTf^-$ radicals are indicated with solid arrows.

increases the concentration of $Br_2^{-•}$, i.e., reaction 10 certainly occurs in this IL system. The relative yields of radicals I and II do not change with dilution of the sample below 1 mol %. At the lowest dilution, resonance lines from $^{*}CF_3$ and $^{*}CF_2SO_2NTf^-$ radicals^{18,21,23} superimpose on the EPR spectra of radicals I and II, as seen in Figure 5b. Only radical I was observed in C_2 mim NTf₂:Br (Figure 6S).

To contrast aliphatic vs aromatic ILs, we examined $P_{14}NTf_2$:Br. In the previous studies,^{19,21} $C(-H)^{+•}$ radicals were identified as the progenitors of the EPR spectra shown in Figure 7a. Varying the bromide concentration does not have strong effect on these spectra. Examination of Figure 7b indicates spectral evolution similar to that observed in C_4 mim NTf₂:Br, with two differences. First, $BrA^{-•}$ is observed even in concentrated 12.6 mol % bromide solution. Second, only one variant of this radical is present, and its $M(Br) = +3/2$ line reveals superhyperfine structure that is likely to originate from the unpaired electron coupling to ^{19}F (as the splitting pattern is similar to the one observed for radical II in C_4 mim NTf₂ and C_4 mim TfO, see above), although the corresponding hfcc is close to that of radical I. Alternatively, this feature may result from the accidental resonance of two $M(Br) = +3/2$ lines in the orientations of the hfc tensor for $^{79,81}Br$ along and perpendicular to the magnetic field B of the EPR spectrometer. As none of the resonance lines for $B \parallel x,y$ can be identified due to the spectral congestion, we cannot choose between these two alternatives.

To summarize this section, radiolysis of bromide solutions in ILs yields stable $BrA^{-•}$ radicals instead of trapped Br^{\bullet} atoms. These radicals persist at low temperature, but at higher temperature exchange reaction 10 takes place. We turn to the photochemistry of these systems.

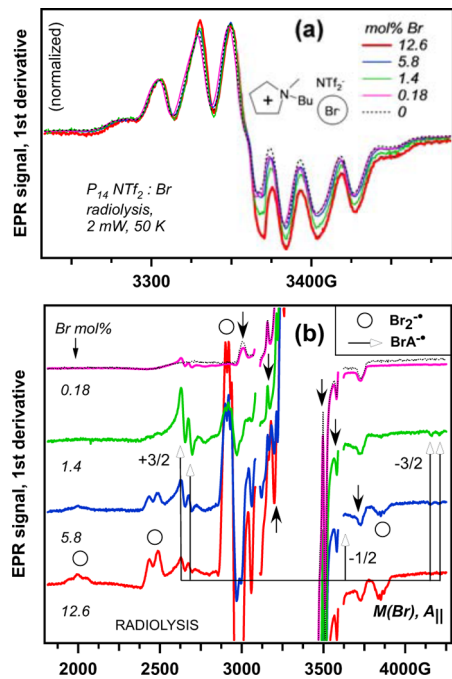


Figure 7. As in Figure 2 for 2.5 MeV electron irradiated $P_{14}NTf_2$. Solid arrows in panel b indicate the resonance lines of ${}^{\bullet}CF_3$ and ${}^{\bullet}CF_2SO_2NTf^{\bullet}$ radicals. Observe that only one ^{19}F -coupled variant of the $BrNTf_2^{\bullet}$ radical is present in this EPR spectrum.

3.3. Photochemistry of Bromide Solutions (355 nm Laser Excitation). In the absence of light-absorbing impurities, 355 nm laser excitation of the chosen IL solvents can only be biphotonic, as these solvent do not have discernible absorption bands in the UVA region.^{15,27} To demonstrate this point, we photolyzed $P_{14}NTf_2$ containing 12.8 mol % $N_{4444}Br$. The latter is a crystalline compound that was multiply recrystallized to ensure the absence of photoactive impurities. Photolysis of neat $P_{14}NTf_2$ yielded no radicals detectable by EPR; as bromide was added, the yield of organic radicals scaled linearly with the bromide concentration (Figure 7S). Figure 8S shows the power dependence for the integrated EPR signal, which (at low microwave power) is directly proportional to the radical yield. This dependence is quadratic in power, proving that the radicals are indeed generated through biphotonic excitation. To demonstrate that this excitation is of, specifically, bromide rather than organic cations, we introduced 10 mol % ClO_4^- and BF_4^- as their crystalline N_{4444}^+ salts (once again utilizing our ability to purify these compounds through recrystallization) into the IL solution. Figure 9S demonstrates the comparisons of the EPR spectra from these three photoirradiated solutions obtained after identical light exposure. While some EPR signals were observed for perchlorate and tetrafluoroborate, the radical yield was 100–150 times lower than in the bromide system. Thus, there is little doubt that the radicals are generated in biphotonic electron detachment from the bromide.

The observed EPR spectrum (Figures 8a and 9) is quite similar to the one observed in radiolysis (Figure 9a),²¹ suggesting that the progenitors of this spectrum are $C(-H)^{\bullet+}$ radicals, and we expected to observe the same BrA^{\bullet} radicals that were observed in radiolysis (section 3.2), reasoning that the Br^{\bullet} atom released in the photoreaction bonds to matrix anions via reaction 7. Figures 8b show the EPR spectrum of

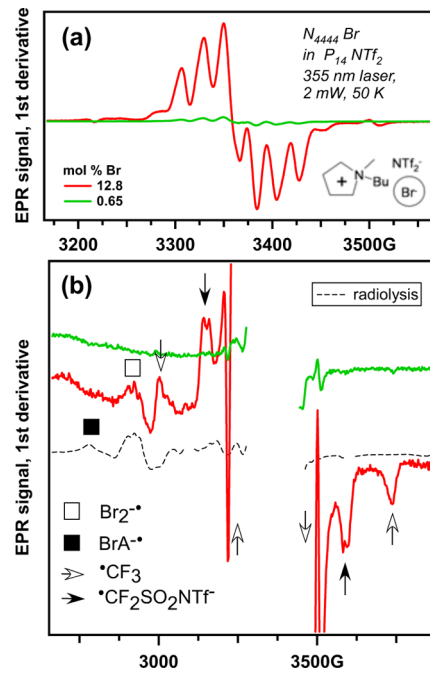


Figure 8. EPR spectra obtained in $P_{14}NTf_2$ containing 0.65 and 12.8 mol % tetrabutyl bromide (green and red traces, respectively) after 355 nm laser photolysis at 77 K (equal exposure times; 50 K, 2 mW). Panel a, 2 G modulation; panel b, 10 G modulation. In panel b, the dashed line is the EPR spectrum of the radiolyzed 12.8 mol % sample. The symbols are given in the inset. No lines from the BrA^{\bullet} radical are observed in the photolyzed samples.

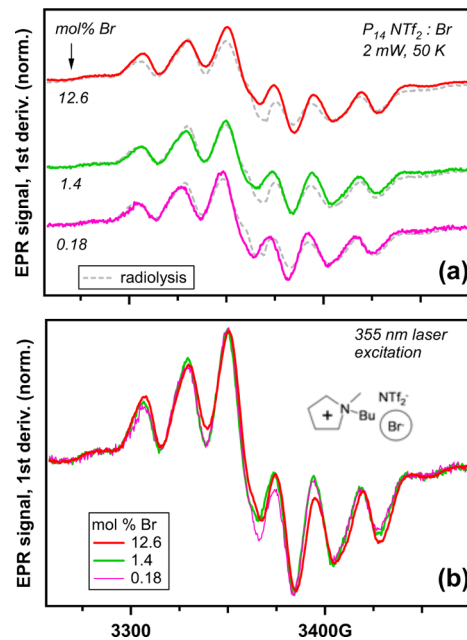
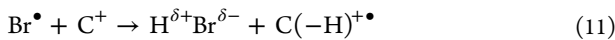


Figure 9. Normalized EPR spectra from bromide-doped $P_{14}NTf_2$ either radiolyzed by 2.5 MeV electrons (dashed lines) or photolyzed using 355 nm laser light (solid lines) at 77 K (2 G, 2 mW). Panel a shows a comparison between the photolyzed and radiolyzed samples, respectively, and panel b shows a comparison of the EPR spectra of photolyzed samples for different bromide concentrations. See the discussion in the text.

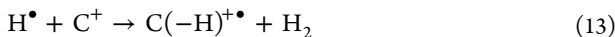
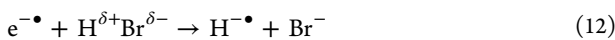
12.8 mol % solution of $N_{4444}Br$ in $P_{14}NTf_2$ scanned across a wider field. Even at this high concentration, the relative yield of

$\text{Br}_2^{\cdot-}$ was quite low. At no concentration of the bromide did we observe the $\text{BrA}^{\cdot-}$ radicals that were readily observed in radiolyzed samples. The same results were obtained for photolysis of P_{14}Br and C_4mimBr in $\text{P}_{14}\text{NTf}_2$ (e.g., Figure 10S). Importantly, the EPR spectrum of organic radicals (Figure 11S) did not strongly depend on bromide's counterion, suggesting that the anion was uniformly dispersed in a solid matrix.

These results could have been interpreted as evidence for photodissociation of C–N or C–H bonds in the P_{14}^+ cation had we not proved above that no organic radicals are formed in the absence of bromide. Furthermore, the $\text{Br}_2^{\cdot-}$ radical was observed in concentrated bromide solutions (albeit, at low yield). The inescapable conclusion is that the photogenerated Br^{\cdot} atom is immediately consumed (unless high concentration of bromide is present so some of these atoms convert to the $\text{Br}_2^{\cdot-}$ radical via reaction 2). However, results given in section 3.2 indicate that Br^{\cdot} atoms ($\text{BrA}^{\cdot-}$ anions) are indefinitely stable in a low-temperature IL matrix once generated. Furthermore, the origin of $\text{C}(-\text{H})^{\cdot+}$ radicals observed in this photolytic reaction (Figure 8a) requires rationalization. In radiolysis, these radicals occur through ionization of cations (followed by their deprotonation). Since no radicals are observed in photolysis of IL solvents without bromide, there are two possible scenarios: either (i) these radicals derive from the electrons that are injected into the solution in reaction 1 or (ii) photogenerated Br^{\cdot} atom abstracts H from the cation

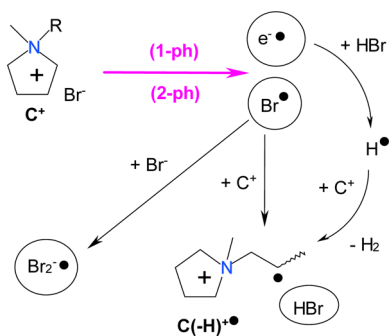


yielding such $\text{C}(-\text{H})^{\cdot+}$ radicals. Scenario (ii) accounts not only for $\text{C}(-\text{H})^{\cdot+}$ radical, but also for lack of the $\text{BrA}^{\cdot-}$ radicals, provided that reaction 11 occurs faster than reaction 7 (but not faster than reaction 2 in concentrated bromide solutions). Scenario (ii) makes possible scenario (i), as the only plausible reaction of the photoelectrons leading to $\text{C}(-\text{H})^{\cdot+}$ radicals is through scavenging of the electrons by the proton centers (as discussed in ref 21) followed by H-abstraction from the cations by the released H^{\cdot} atoms (see Scheme 1)



It appears that to explain the sum total of our EPR results, it is necessary to postulate the occurrence of rapid reaction 11.

Scheme 1. Summary of Photochemistry of Bromide in Aliphatic ILs^a



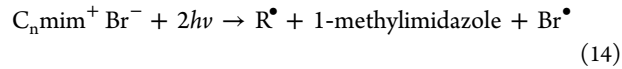
^a"1-ph" and "2-ph" designate 1-photon and 2-photon excitation, respectively.

As explained in section 3.2, radiolysis does not oxidize bromide directly; the oxidation occurs through reaction 8 that necessarily yields the $\text{BrA}^{\cdot-}$ radical; in this sense photolysis is not equivalent to radiolysis. (This has precedent in radiolysis of aqueous bromide solutions, where radiation generates HO^{\cdot} radicals that react with Br^- to yield BrOH^{\cdot} radicals that subsequently react with another bromide to yield $\text{Br}_2^{\cdot-}$.¹³ the hydrated Br^{\cdot} atom is not generated in radiolysis, while it is formed in reaction 1). Likewise, only photolysis yields Br^{\cdot} atoms in ILs, and these atoms can be converted to $\text{BrA}^{\cdot-}$ radicals in reaction 7 only if there is no reaction that is faster than reaction 11. In ILs, reaction 11 appears to be the fastest reaction of Br^{\cdot} atoms.

Radiolytic oxidation of the IL cations might produce a different mixture of $\text{C}(-\text{H})^{\cdot+}$ radicals than reaction 11, as the former is determined by the energetics of C^{2+} deprotonation, while the latter is dictated by the energetics of C–H bonds.²¹ There are reasons to expect that the former reaction favors terminal and penultimate C-centered radicals, while the latter favors abstraction from α -carbons.^{19,21} There are indeed differences between the EPR spectra of $\text{C}(-\text{H})^{\cdot+}$ radicals obtained in 355 nm laser photolysis and radiolysis (Figure 9a) and also of the EPR spectra obtained in 355 nm laser photolysis of 12.8 mol % solution vs 0.2 and 1.4 mol % solutions (Figure 9b), though the differences are too small to amount to conclusive proof that site-specific H-abstraction occurs in 355 nm photolysis of dilute solutions.

Turning to aromatic ILs, we examined the $\text{C}_n\text{mim NTf}_2:\text{Br}$ system. Unlike $\text{P}_{14}\text{NTf}_2$, 355 nm laser photolysis of $\text{C}_n\text{mim NTf}_2$ yields radicals observable by EPR, though the yield is very low, and the resulting EPR spectrum strongly resembles the EPR spectra observed in radiolysis of the same IL (Figures 12S). Addition of bromide greatly increases the radical yield (e.g., Figure 10a,b). Another similarity is that as in the $\text{P}_{14}\text{NTf}_2:\text{Br}$ system, no $\text{BrA}^{\cdot-}$ radicals were observed in dilute solutions, and only $\text{Br}_2^{\cdot-}$ radicals were observed in concentrated solutions (Figure 10c). A most spectacular difference, however, is observed in the spectra of organic radicals derived from the cations (Figure 11). In radiolysis of $\text{C}_4\text{mim NTf}_2:\text{Br}$ solutions (section 3.2), the predominant feature is C^{\cdot} and C_2^{2+} radicals (Figure 5). In 355 nm photolysis of $\text{C}_4\text{mim Br}$ (section 3.1), the yield of C^{\cdot} was reduced, and methyl and alkyl radicals were observed (Figure 1), which indicates fragmentation of C^{\cdot} radical generated in the photoreaction. We can now recognize that some of these alkyl radicals may, in fact, be the $\text{C}(-\text{H})^{\cdot+}$ radicals generated through reaction 11. The relative yield of these radicals remains high even at dilution, as most of the photogenerated bromine atoms decay in reaction 11. As shown in Figure 11, this is indeed the case: as bromide becomes more dilute, the relative fraction of C_2^{2+} radical does not increase. Only when there is no bromide, the biphotonic excitation yields EPR spectra resembling of the ones obtained in radiolysis. Interestingly, methyl elimination is observed only in neat $\text{C}_n\text{mim Br}$, whereas no such photoreaction occurs in $\text{C}_n\text{mim NTf}_2:\text{Br}$ solutions (Figures 12S and 11).

We conclude that absorption of two photons by the bromide in imidazolium ILs causes an overall photoreaction that can be written as



where R^{\cdot} stands for the eliminated terminal radical. Reaction 14 is followed by rapid reactions 2 and 7.

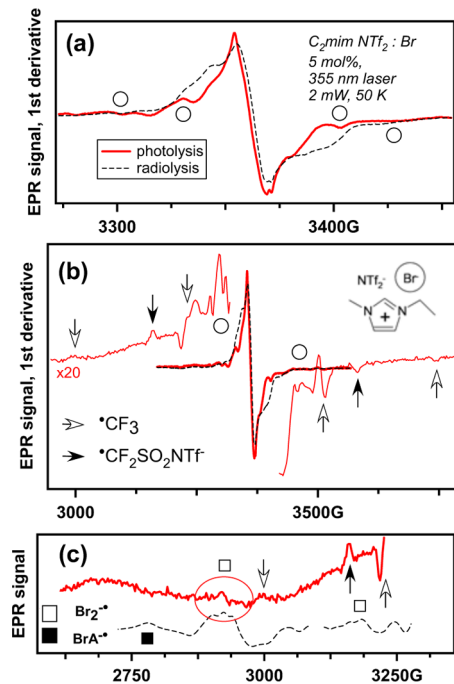


Figure 10. EPR spectra observed in 355 nm laser photolysis of $C_4\text{mim NTf}_2\text{:Br}$ containing 5 mol % bromide. In panel a, we compare the spectrum with one for a radiolyzed sample (dashed line). The resonance lines of $C(-\text{H})^{\bullet\bullet}$ radicals are indicated by open circles. In panel b, the resonance lines of ${}^*\text{CF}_3$ and ${}^*\text{CF}_2\text{SO}_2\text{NTf}^-$ radicals are indicated with open and filled arrows, respectively. In panel c, the EPR spectrum is again compared with the EPR spectrum of a radiolyzed sample that exhibits both $\text{Br}_2^{\bullet\bullet}$ and $\text{BrA}^{\bullet\bullet}$ radicals (open and filled squares, respectively). Only a weak $M(2\text{Br}) = +1$ resonance line of $\text{Br}_2^{\bullet\bullet}$ is observed in the EPR spectrum of the photolyzed sample.

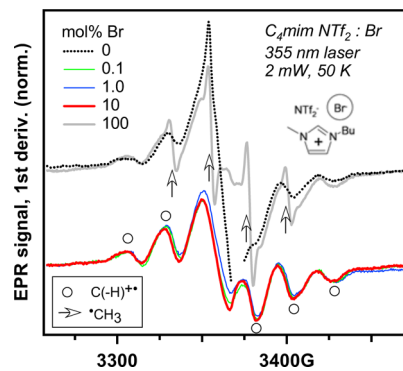


Figure 11. EPR spectra observed in 355 nm laser photolysis of $C_4\text{mim NTf}_2\text{:Br}$ containing different concentrations of bromide. In panel a, we compare the spectrum with one for a radiolyzed sample (dashed line). The resonance lines of R^{\bullet} and $C(-\text{H})^{\bullet\bullet}$ radicals are indicated by open circles, and open arrows indicate the resonance lines of the methyl radical.

3.4. One-Photon Excitation. This brings us to one-photon photooxidation of bromide in ILs. No evidence for one-photon generation of radicals in low-power 266 nm excitation or UV lamp photolysis (>250 nm) of $P_{14}\text{ NTf}_2\text{:Br}$ was obtained. Exposure of the sample to 200–220 nm light of the UV lamp did result in a very slow (over 80 min) buildup of the EPR spectrum for 12.6 mol % bromine solution shown in Figure 12a. The EPR signal was too weak to attempt the detection of Br-related radicals, but the lines of the $C(-\text{H})^{\bullet\bullet}$ radical were

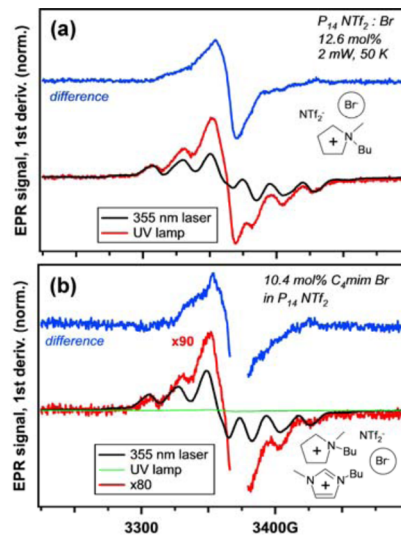


Figure 12. Normalized EPR spectra obtained in 355 nm laser photolysis and UV lamp photolysis of (a) 12.6 mol % $P_{14}\text{Br}$ in $P_{14}\text{NTf}_2$ and (b) 10.4 mol % $C_4\text{mim Br}$ in $P_{14}\text{NTf}_2$ (see the legend). Plotted at the top of each panel is the difference trace. The resonance line of the E' center in the silica sample tube is excluded from the plot.

clearly present, in addition to a structureless singlet of uncertain origin. The quantum yield of this photoreaction must be extremely low ($<10^{-3}$). A similar species was observed in UV lamp photolysis of $C_4\text{mim Br}$ solutions in $P_{14}\text{ NTf}_2$.

The situation for aromatic IL matrixes is different, as these have charge-transfer bands that, in principle, can provide a reaction channel for photoinduced reactions 5a and/or 5b. To address this possibility, we irradiated $C_n\text{mim NTf}_2\text{:Br}$ samples using >240 nm photons from the UV lamp (to eliminate any possibility of 2-photon excitation); see Figure 13a. Exactly the same EPR spectra were obtained in low-power 266 nm photoexcitation. The normalized EPR spectra do not evolve as a function of $[\text{Br}^-]$ for dilute solutions (Figure 13b) and strongly resemble the EPR spectra observed in radiolysis of neat $C_n\text{mim NTf}_2$, with the $C_2^{\bullet\bullet}$ and $C(-\text{H})^{\bullet\bullet}$ radicals both contributing to the EPR spectrum (Figure 13b). While the addition of bromide transformed $C_2^{\bullet\bullet}$ to C^{\bullet} in radiolysis (Figure 5a), no such transformation was apparent in UV photolysis (Figure 13a). Because of the low radical yield, detection of Br-derived radicals presented technical difficulty; still, no evidence for the presence of $\text{BrA}^{\bullet\bullet}$ radicals was obtained (Figure 13S), except for 10 mol % bromide solution, for which there was a hint of $M(\text{Br}) = +1$ line of $\text{Br}_2^{\bullet\bullet}$ present in the EPR spectrum, but the signal-to-noise ratio is one (Figure 14S).

The simplest explanation of these results is that the Br^{\bullet} atom was generated either via reaction 1 or reaction 5, producing a geminate pair involving the $C_2^{\bullet\bullet}$ radical. There is a competition of reactions 2 and 11 (Scheme 2). Unless the concentration of bromide is high, H-atom abstraction prevails, and the Br^{\bullet} atom is entirely converted to $C(-\text{H})^{\bullet\bullet}$ radicals. At high concentration of bromide, some $\text{Br}_2^{\bullet\bullet}$ radicals are generated. The efficiency of charge separation is very low.

3.5. Bromine Atom Reactivity. Our suggested mechanism hinges on a seemingly unlikely proposition that, even at 77 K, bromine atoms are so reactive that they can abstract H atom from the alkyl arms of the IL cations in preference to $\text{Br}_2^{\bullet\bullet}$ formation (even in concentrated bromide solutions). In

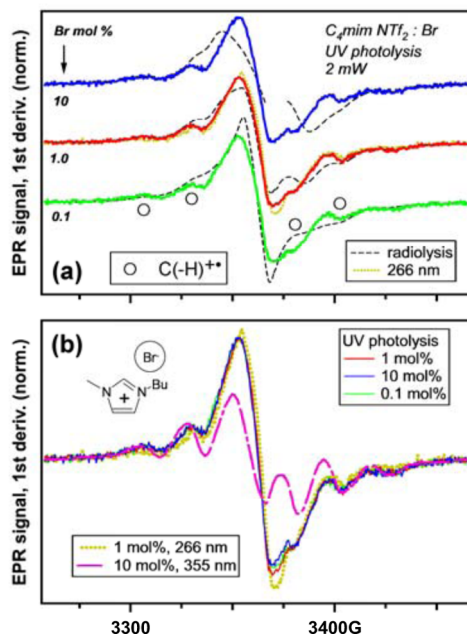
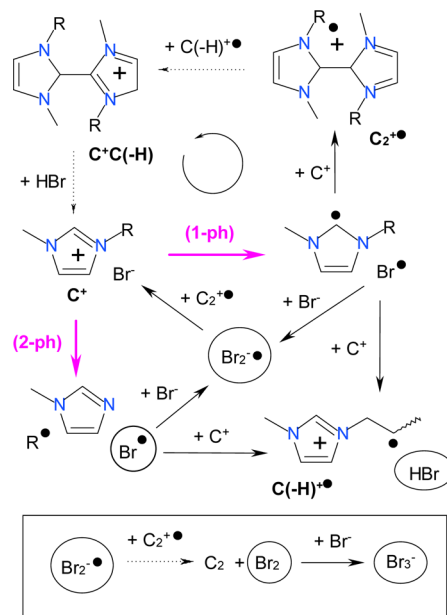


Figure 13. (a) Normalized EPR spectra obtained in UV lamp photolysis (solid lines) and radiolysis (dashed lines) of $\text{C}_4\text{mim NTf}_2\cdot\text{Br}$ at 77 K (see the trace labels for bromide concentrations). The resonance lines of R^\bullet and $\text{C}(-\text{H})^{\bullet+}$ radicals are indicated by open circles. The same scaled traces for UV photolysis are replotted in panel b. EPR spectra obtained in 266 nm (8 J/cm^2) and 355 nm (0.12 J/cm^2) laser photolysis of 1 mol % and 10 mol % bromide systems, respectively, are superimposed on these traces (see the legends in the plots).

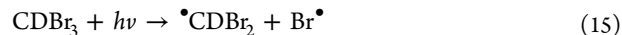
Scheme 2. Summary of Photochemistry of Bromide in Aromatic ILs^a



^aHypothetical reactions are indicated by dashed arrows. "1-ph" and "2-ph" designate 1-photon and 2-photon excitation, respectively.

biphotonic excitation, one can expect that the released bromine atom has excess kinetic or electron² energy to facilitate reaction 11, but this appears unlikely for one-photon excitation. Since postulated reaction 11 should occur regardless of the source of

the Br^\bullet atoms, we sought an alternative way of producing such atoms. To this end, we photolyzed deuterobromoform



that yields a pair that subsequently recombines yielding CDBr_3 and/or $\text{Br}-\text{Br}$ bound isomer.³⁸ UV lamp photolysis of neat CDBr_3 and 1 mol % solution in methylcyclohexane yield a strong signal from the $\cdot\text{CDBr}_2$ radical with $g = (2.072, 2.0075, 2.005)$ and $A(\text{Br}^\bullet) = (-40, 0, +105) \text{ G}$ (Figures 15S and 16S), and the same species is observed in 355 nm laser photolysis of neat CDBr_3 (this compound still absorbs at 355 nm, which is the very red edge of the absorption band). We photolyzed 4 and 28 mol % solutions in $\text{P}_{14}\text{NTf}_2$. The lines from $\cdot\text{CDBr}_2$ superimposed on the lines of $\text{C}(-\text{H})^{\bullet+}$ radicals (Figure 14a)

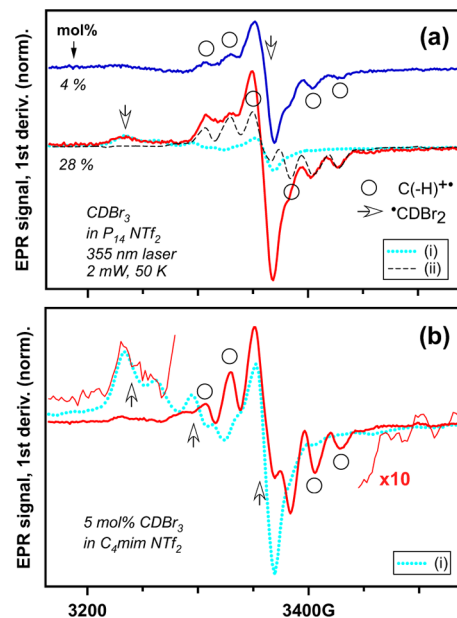


Figure 14. EPR spectra of (a) 4 and 28 mol % deuterobromoform in $\text{P}_{14}\text{NTf}_2$ and (b) 5 mol % deuterobromoform in $\text{C}_4\text{mim NTf}_2$. In both EPR spectra, in addition to the resonance lines of the $\cdot\text{CDBr}_2$ radical indicated by the arrows (see Figure 15S in the Supporting Information), there are also resonance lines from $\text{C}(-\text{H})^{\bullet+}$ radicals indicated by the open circles. For comparison, the spectrum of the latter radicals as observed in 355 nm laser photolysis of $\text{P}_{14}\text{NTf}_2$ is shown by dashed line. In both of these concentrated solutions, most of the 355 nm excitation light is absorbed by the CDBr_3 .

and no BrA^\bullet radicals were observed. The same result was obtained for photodissociation of CDBr_3 in $\text{C}_4\text{mim NTf}_2$ (Figure 14b). Thus, this method of producing Br^\bullet atoms also resulted in a species undergoing reaction 11. We conclude that little or no activation is required to facilitate reaction 11 in ILs, even under cryogenic conditions.

4. DISCUSSION

4.1. X[•] Atoms and XA^\bullet Radicals. In polar solvents, Br^\bullet atom abstracts hydrogen from alkyl groups with reaction rates^{39,40} ranging between $(1-5) \times 10^4 \text{ M}^{-1} \text{ s}^{-1}$ (for primary hydrogens) and $10^8 \text{ M}^{-1} \text{ s}^{-1}$ (ternary hydrogens); these rates can be compared with $10^{10} \text{ M}^{-1} \text{ s}^{-1}$ for reaction 2 in water¹³ and $1.5 \times 10^{10} \text{ M}^{-1} \text{ s}^{-1}$ in acetonitrile.⁴¹ The hydrogen abstraction accelerates dramatically when the Br^\bullet atom can oxidize the substrate before the abstraction ($3 \times 10^{10} \text{ M}^{-1} \text{ s}^{-1}$ for triethylamine and *p*-cresol in acetonitrile),⁴⁰ when

weakened C–H bonds in alkylaryl groups are involved ($10^8 \text{ M}^{-1} \text{ s}^{-1}$)³⁹ or a π -complex is formed ($1.6 \times 10^8 \text{ M}^{-1} \text{ s}^{-1}$ for pyridine in CCl_4).⁴¹ That trapped Br^\bullet atoms in ILs can eventually abstract H from cations is not surprising; the surprising observation (section 3) is the facility of reaction 11 compared to BrA^\bullet and Br_2^\bullet formation, even in a low temperature IL matrix.

BrX^\bullet ($X = \text{Br}, \text{SCN}$) radicals are well-known in aqueous bromide chemistry,^{13,31–33} and Br -succinimide[–] anion was observed in radiolysis of *N*-bromosuccinimide.³⁶ In Table 4S, we used gas phase DFT energetics (Tables 2S and 3S) to obtain estimates for bond energies and structural and magnetic parameters for geometry optimized BrA^\bullet radicals. The estimate for Br–Br bond energy in Br_2^\bullet is 1.62 eV, which is in accord with experimental estimates.¹³ Br–N bond energies for BrA^\bullet radicals involving succinimide, dicyanamide, and bistriflimide are 1.24, 1.06, and 0.61 eV, respectively, and the Br–O bond energy in the triflate complex is 0.65 eV. All of these energies are significantly greater than 0.1–0.2 eV for the gas-phase $\text{Br}^\bullet\cdots\text{OH}_2$ complex estimated by Jungwirth and co-workers¹¹ and 0.15 eV by Li et al.¹² While such complexation occurs in molecular solvents, the effect is exacerbated in ILs, as matrix anions bond to polarizable bromine atom much more strongly than neutral molecules. Another import from Table 4S is that in all cases, reaction 8 is more exergonic than reaction 7. Facility of the latter reaction accounts for the efficient generation of BrA^\bullet radicals in radiolysis (section 3.2). Another consideration is the potential involvement of BrX^\bullet radicals in exchange reactions 10 and



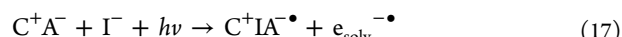
Table 5S gives the calculated enthalpies for reaction 10 for DCA^- and NTf_2^- . In both cases, the exchange is exergonic by >0.56 eV, which rationalizes the observed conversion of BrA^\bullet to Br_2^\bullet upon warming of the irradiated samples (section 3.2). As for reaction 16 (that is known to occur for thiocyanate),^{32,33} the energetics are prohibitive: the $^\bullet\text{NTf}_2$ radical is not known to form A_2^\bullet dimers at all due to steric hindrance,¹⁸ whereas the N–N bond in the A_2^\bullet dimer radical anion of diacyanamide¹⁷ is too weak (Table 3S), and reaction 16 is endothermic by 0.67 eV. Once the bromine atom is locked in the BrA^\bullet radical, it cannot be released unless it reacts with a bromide or, possibly, a reactive bromine species.

These DFT calculations indicate that the Br–N bond in the BrA^\bullet radicals for imide anions is significantly elongated as compared to those in corresponding *N*-bromoimides (2.5–2.7 Å vs 1.85–1.91 Å) and suggest (Table 4S) that the same BrA^\bullet radicals can be generated by electron addition reaction 6, as neutral BrA molecules have large electron affinities in the gas phase (2.2–3.9 eV). Such a reaction was indeed observed for *N*-bromosuccinimide.³⁶ For the latter, the calculated hfccs on bromine-79 and nitrogen-14 agree reasonably well with the ones determined experimentally (Table 6S and 7S), except for the isotropic constant in ⁷⁹Br. As seen from Table 7S, this is not an isolated discrepancy, and it illustrates difficulty of estimating electron density in many-electron polarizable atoms; for low-Z elements, the estimates are more reliable. These DFT calculations indicate significant spin density on heteroatom nuclei that are bonded to bromine. Observations of super-hyperfine structure in BrA^\bullet radicals (section 3.2) constitute the sufficient proof that bromine atom is bound to these anions. The experimental estimates for longitudinal components of the hfcc tensors for ⁷⁹Br nuclei broadly agree with the calculated

parameters in Table 7S, and so does the estimate for the $A_{||}(^{14}\text{N})$ component for BrDCA^\bullet .

As mentioned in the Introduction, radiolysis of $\text{C}_n\text{mim Cl}$ does not yield observable chlorine related radicals, suggesting that the released Cl^\bullet atoms abstract hydrogen from cations faster than they form Cl_2^\bullet (even in the neat IL). As shown in section 3, the released Br^\bullet atoms also rapidly abstract hydrogen from the cations; this reaction is faster than BrA^\bullet formation in dilute bromide solutions in $\text{C}_n\text{mim A}$, but not faster than Br_2^\bullet formation in concentrated $\text{C}_n\text{mim A:Br}$.

Given the low energy of the H–I bond, it is almost certain that this H-abstraction does not occur for iodine atoms, even if these species are generated with excess energy. This is also suggested by experiments of Katoh et al.²⁷ using dilute (2 mM) iodide solutions in $\text{N}_{1113}\text{NTf}_2$. Had all the I^\bullet atoms released in reaction 1 reacted with cations, no delayed formation of I_2^\bullet could be observed. This, however, does not imply that solvated I^\bullet atoms persist in this IL, as the iodine atoms can form IA^\bullet radicals that slowly convert to I_2^\bullet radicals through a reaction analogous to reaction 10. Given the general propensity of halide atoms to form complexes, this almost certainly is the case. We, therefore, suggest that for the iodide in aliphatic ILs, the correct photoreaction is not reaction 1 but



Returning to the question regarding why Br^\bullet atoms H-abstraction is more facile than reaction 7, two possible answers are that (i) such atoms are photogenerated hot and (ii) solvation effects in the ILs make dramatic changes to the energetics of H-abstraction as compared to both the gas phase and molecular solvents. While we cannot entirely exclude (i) in two-photon excitation of bromide, it seems unlikely that such hot atoms are also generated in one-photon photolysis (section 3.4) and low-energy photodissociated bromoform (section 3.5). It appears that reaction 11 proceeds even with thermalized Br^\bullet atoms. In polar molecular solvents, the released HBr molecule is associated.^{38,39} The driving force for reaction 11 in ILs might be provided by sharing of the proton by Br^- and A^- anions. Theoretical modeling of this reaction is beyond the scope of this article.

4.2. Photoinduced Charge Separation: General Outlook. Our results are consistent with the occurrence of reaction 1 in aliphatic ILs with the added insight that the released Cl^\bullet and Br^\bullet atoms rapidly abstract H from the cation. The occurrence of this photoreaction in aromatic ILs remains undecided as all of our observations can be interpreted either as electron ejection followed by rapid electron attachment or as photoinduced charge transfer (reactions 5a and 5b). Likewise, the dissociation of the cation observed in 2-photon excitation of bromide in ILs (section 3.3) can be interpreted either as (i) C–N cleavage in the corresponding excited state of C^\bullet radical generated in charge transfer or (ii) an example of DEA involving prethermalized electron. The choice between these alternatives hinges on the nature of a broad absorbance that is observed in the ultrafast laser experiments^{24–29} that can originate either (i) from $s \leftarrow p$ transition of a cavity-like electron (or some other s-like delocalized excess electron state) or (ii) $\sigma \leftarrow \sigma^*$ transition in the C_2^\bullet radical. The latter¹⁷ is but a specific realization of charge delocalization at the site of anion vacancy, and the two scenarios do not necessarily contradict each other, as the solvated electron can always be viewed as a

solvent-supported multimer ion, as the wave function of the cavity electron is composed of the protruding antibonding orbitals of several cations.^{24,28} Satisfactory clarification of these details requires further ultrafast studies.

Regardless of these details, shortly after the halide excitation (<100 ps) the geminate pair generated in $C_n\text{mim}^+$ A^-X solutions evolves from the original (C^\bullet , X^\bullet) pair to ($C_2^{+\bullet}$, $C(-H)^{+\bullet}$) pair (in dilute solutions) or ($C_2^{+\bullet}$, $X_2^{-\bullet}$) pair (in concentrated solutions). In addition to back recombination



the latter pair can potentially recombine, yielding neutral products



and the resulting dihalide can promptly react with the halide anion to yield X_3^- anion



In aqueous photo-CTTS reactions,⁹ X_3^- is generated through disproportionation of $X_2^{-\bullet}$ radicals

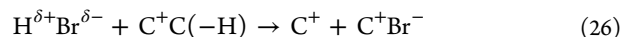
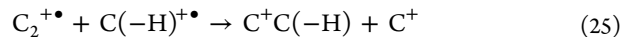


or in reactions of X^\bullet atoms:



The latter reaction provides X_2 feed for reaction 21. Therefore, in polar solvents, all reaction pathways leading to X_3^- involve cross-recombination of radicals, and the formation of X_3^- can only occur on a long time scale controlled by the diffusion of radicals.⁹ In contrast, in ILs the formation of X_3^- can occur on a shorter time scale, as X_2 and X_3^- can be photogenerated via reaction 20 followed by reaction 21. As our study indicates, X^\bullet atoms are rapidly converted to HX, so there are no alternative pathways (reactions 23 and 24) to the formation of X_3^- . Hence, the detection of X_3^- on a short time scale, in the low excitation regime (before the secondary radical chemistry becomes important) can serve as indication for the occurrence of reaction 21. That X_3^- is present in the photolysate and radiolysate has been demonstrated by electrospray mass spectrometry; unfortunately, product analysis cannot distinguish between geminate vs cross-recombination. A more direct, time-resolved method can settle this matter. Efficient photogeneration of X_3^- has ramifications for long-term photodarkening of ILs, as this species strongly absorbs UV light and has rich photochemistry; it is also a potent halogenation agent. Thus, the occurrence of irreversible reaction 20 would have significant impact on long-term photostability of halide-doped ILs.

In dilute bromide solutions, the primary photoreaction yields HBr as the only brominated product, and the radical pair is either $C_2^{+\bullet}$ and $C(-H)^{+\bullet}$ (1-photon excitation) or R^\bullet and $C(-H)^{+\bullet}$ (2-photon excitation). The latter pair can recombine or disproportionate, whereas the former can only disproportionate to C^+ and $C^+C(-H)$. The latter species is the known product of the attachment of *N*-heterocyclic carbene, $C(-H)^{\bullet\dagger}$, to the parent cation C^+ at carbon-2; this metastable product is involved in the well-known Lemal equilibria of the carbenes⁴² shown in Scheme 3S (see also the discussion in ref 20). We suggest that back reaction follows the sequence (Scheme 1)

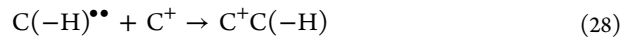


that completes the photochemical cycle. Photolytic degradation of the IL is still possible through the secondary reactions of escaped radicals, e.g., via recombination of $C(-H)^{+\bullet}$ (that was observed in radiolysis of ILs).^{19,30}

EPR spectroscopy that we used in this study is selective to open-shell species, and a photochemical reaction that produces closed-shell reactive intermediates (and only such intermediates) would escape EPR detection. The only such bond-breaking photoreaction in our system would be deprotonation of the cation^{20,42}

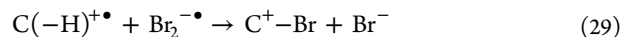


In ILs, $C_n\text{mim}^+$ cation is marginally bound even in the ground state,²⁰ and it readily deprotonates upon the addition of weak bases to yield *N*-heterocyclic carbene, $C(-H)^{\bullet\dagger}$.⁴² The latter species is known to react with the parent cation (Scheme 3S)



yielding the same product as reaction 25.⁴² Regardless of whether the main photoreaction is charge separation (reaction 5b) or deprotonation (reaction 27), shortly after the excitation event the same photolytic products, $C^+C(-H)$ and HBr, are generated (that subsequently undergo reaction 26). The only difference, product wise, is the formation of cross-recombination products involving the escaped $C_2^{+\bullet}$ and $C(-H)^{+\bullet}$ radical cations.

In dilute aliphatic ILs, $C(-H)^{+\bullet}$ radicals are generated from both radical partners (Scheme 2), and the subsequent chemistry involves recombination and disproportionation of such radicals. In more concentrated solutions, $Br_2^{-\bullet}$ radicals are formed, and radical bromination of $C(-H)^{+\bullet}$ radicals may occur (in the aliphatic arm),



to generate Br-substituted cations.

5. CONCLUSIONS

Schemes 1 (for aliphatic ILs) and 2 (for aromatic ILs) summarize our results.

Photo-CTTS reaction 1 provides a convenient reference point for understanding the photochemistry of halide (X^-) anions in ILs, but the latter has distinct features that limit the usefulness of the analogy. With the exception of iodide, the released halogen atom promptly abstracts H from the aliphatic arms of the IL cations; a competing reaction is the formation of dihalide radical anions. No $\sigma^2\sigma^{*1}$ bound $BrA^{-\bullet}$ radicals involving IL anions (A^-) were photolytically generated, although such radicals readily form in radiolysis of the same IL solutions. We directly observed such $BrA^{-\bullet}$ radicals using EPR and modeled them using density functional theory. The hydrogen abstraction by photogenerated Br^\bullet atoms is so rapid that such binding to IL anions does not occur in photolysis. The cause for this unexpected facility of H abstraction in ILs is unknown, but our experiments suggest that the involvement of hot bromine atoms is unlikely. For iodine atoms, this H abstraction does not occur; it is likely that $IA^{-\bullet}$ radical anions form instead. We showed that such $XA^{-\bullet}$ radicals convert to $X_2^{-\bullet}$ radicals in a thermally activated reaction 10 with the progenitor X^- anion.

The H abstraction by bromine atom occurs both in 1- and 2-photon excitations of bromide in ILs. In 2-photon ionization of bromide (355 nm) in imidazolium ILs, the charge transfer is concerted with the elimination of long arms from the cation, yielding terminal alkyl radicals. The quantum yield of 1-photon induced charge transfer (220–240 nm) in the same system is quite low ($<10^{-3}$) and results in the formation of HBr, the dimer radical cation, $C_2^{+}\bullet$, and H-loss radical, $C(-H)^{+}\bullet$. In concentrated bromide solutions, $Br_2^{-}\bullet$ radical is also generated. We speculate (section 4.2) that the latter species is converted to Br_3^{-} on a short time scale (reaction 20) and that X_3^{-} anions play an important role in the long term photodegradation of ILs. We also suggest that disproportionation of geminate partners generated in dilute IL solutions completes the photochemical cycle (yielding the same cation-derived products as deprotonation) and the photodegradation of such IL systems occurs through cross-reactions of escaped radicals.

ASSOCIATED CONTENT

Supporting Information

List of reactions and abbreviations, Tables 1S to 10S reporting magnetic parameters and energetics, and Figures 1S to 16S with captions, including the experimental EPR spectra, and references given in the tables. This material is available free of charge via the Internet at <http://pubs.acs.org>.

AUTHOR INFORMATION

Corresponding Author

(I.A.S.) Tel: 630-252-9516. E-mail: shkrob@anl.gov. (R.A.C.) Tel: 631-344-4515. E-mail: crowell@bnl.gov. (J.F.W.) Tel: 631-344-4327. E-mail: wishart@bnl.gov.

Notes

The authors declare no competing financial interest.

ACKNOWLEDGMENTS

I.A.S. thanks K. Quigley and R. Lowers for technical support. The work at Argonne and Brookhaven was supported by the US-DOE Office of Science, Division of Chemical Sciences, Geosciences, and Biosciences under contracts Nos. DE-AC02-06CH11357 and DE-AC02-98CH10886, respectively. Programmatic support via a DOE SISGR grant “An Integrated Basic Research Program for Advanced Nuclear Energy Separations Systems Based on Ionic Liquids” is gratefully acknowledged.

REFERENCES

- Chen, X.; Bradforth, S. E. The Ultrafast Dynamics of Photodetachment. *Annu. Rev. Phys. Chem.* **2008**, *59*, 203–231.
- Kloepfer, J. A.; Vilchiz, V. H.; Lenchenkov, V. A.; Bradforth, S. E. Femtosecond Dynamics of Photodetachment of the Iodide Anion in Solution: Resonant Excitation into the Charge-Transfer-To-Solvent State. *Chem. Phys. Lett.* **1998**, *298*, 120–128. Vilchiz, V. H.; Kloepfer, J. A.; Germaine, A. C.; Lenchenkov, V. A.; Bradforth, S. E. Map for the Relaxation Dynamics of Hot Photoelectrons Injected into Liquid Water via Anion Threshold Photodetachment and above Threshold Solvent Ionization. *J. Phys. Chem. A* **2001**, *105*, 1711–1723. Kloepfer, J. A.; Vilchiz, V. H.; Lenchenkov, V. A.; Chen, X.; Bradforth, S. E. Time-Resolved Scavenging and Recombination Dynamics from Ie^- -Caged Pairs. *J. Chem. Phys.* **2002**, *117*, 766–778. Chen, X.; Suffern, D.; Bradforth, S. E. Electron Photodetachment from Aqueous Anions. 2. Ionic Strength Effect on Geminate Recombination Dynamics and Quantum Yield for Hydrated Electron. *J. Phys. Chem. A* **2004**, *108*, 10414–10425. Moskun, A. C.; Bradforth, S. E.; ThØgersen, J.; Keiding, S. Absence of a Signature of Aqueous $I_{(2P_{1/2})}$ after 200-nm

Photodetachment of I^- (aq). *J. Phys. Chem. A* **2006**, *110*, 10947–10955.

(3) Iglev, H.; Laenen, R.; Laubereau, A. Femtosecond Dynamics of Electron Photodetachment of the Fluoride Anion in Liquid Water. *Chem. Phys. Lett.* **2004**, *389*, 427–432. Iglev, H.; Trifonov, A.; Thaller, A.; Buchvarov, I.; Fiebig, T.; Laubereau, A. Photoionization Dynamics of an Aqueous Iodide Solution: The Temperature Dependence. *Chem. Phys. Lett.* **2005**, *403*, 198–204. Fischer, M. K.; Laubereau, A.; Iglev, H. Femtosecond Electron Detachment of Aqueous Bromide Studied by Two and Three Pulse Spectroscopy. *Phys. Chem. Chem. Phys.* **2009**, *11*, 10939–10944.

(4) Doan, S. C.; Schwartz, B. J. Nature of Excess Electrons in Polar Fluids: Anion-Solvated Electron Equilibrium and Polarized Hole-Burning in Liquid Acetonitrile. *J. Phys. Chem. Lett.* **2013**, *4*, 1471–1476. Bragg, A. E.; Kanu, G. U.; Schwartz, B. J. Nanometer-Scale Phase Separation and Preferential Solvation in THF–Water Mixtures: Ultrafast Electron Hydration and Recombination Dynamics Following CTTS Excitation of I^- . *J. Phys. Chem. Lett.* **2011**, *2*, 2797–2804. Xia, C.; Peon, J.; Kohler, B. Femtosecond Electron Ejection in Liquid Acetonitrile: Evidence for Cavity Electrons and Solvent Anions. *J. Chem. Phys.* **2002**, *117*, 8855–8866. Chandrasekhar, N.; Krebs, P.; Unterreiner, A.-N. One-Photon Photodetachment of I^- in Glycerol: Spectra and Yield of Solvated Electrons in the Temperature Range 329 K–536 K. *J. Chem. Phys.* **2006**, *125*, 164512.

(5) Dogel, S.; Freyland, W.; Hippler, H.; Nattland, D.; Chandrasekhar, N.; Unterreiner, A.-N. Ultrafast Dynamics of Excess Electrons in a Molten Salt: Femtosecond Investigation of K–KCl Melts. *Phys. Chem. Chem. Phys.* **2003**, *5*, 2934–2937. Brands, H.; Hippler, H.; Chandrasekhar, N.; Unterreiner, A.-N. Ultrafast Dynamics of Excess Electrons in Molten Salts: II. Femtosecond Investigations of Na–NaBr and Na–NaI Melts. *Phys. Chem. Chem. Phys.* **2005**, *7*, 3963–3969. Chandrasekhar, N.; Endres, F.; Unterreiner, A.-N. Ultrafast Dynamics of Excess Electrons in Molten Salts: Part III. Formation of Solvated Electrons in Room Temperature Ionic Liquids. *Phys. Chem. Chem. Phys.* **2006**, *8*, 3192–3196. Chandrasekhar, N.; Unterreiner, A.-N. Relaxation Dynamics upon Ultrashort UV Photo-Excitation of an Iodide Doped Ionic Liquid and of a Pure Lithium Iodide Melt. *Z. Phys. Chem.* **2006**, *220*, 1235–1246. Chandrasekhar, N.; Unterreiner, A.-N. Time-Resolved Polaron Dynamics In Molten Solutions Of Cesium-Doped Cesium Iodide. *J. Chem. Phys.* **2007**, *127*, 184509.

(6) Sauer, M. C., Jr.; Crowell, R. A.; Shkrob, I. A. Electron Photodetachment from Aqueous Anions. 1. Quantum Yields for Generation of Hydrated Electron by 193 and 248 nm Laser Photoexcitation of Miscellaneous Inorganic Anions. *J. Phys. Chem. A* **2004**, *108*, 5490–5502. Sauer, M. C., Jr.; Shkrob, I. A.; Lian, R.; Crowell, R. A.; Bartels, D. M.; Lian, R.; Oulianov, D. A.; Crowell, R. A.; Shkrob, I. A.; Chen, X.; Bradforth, S. E. Electron Photodetachment from Aqueous Anions. 3. Dynamics of Geminate Pairs Derived from Photoexcitation of Mono- vs Polyatomic Anions. *J. Phys. Chem. A* **2006**, *110*, 9071–9078. Crowell, R. A.; Lian, R.; Shkrob, I. A.; Bartels, D. M.; Chen, X.; Bradforth, S. E. Ultrafast Dynamics for Electron Photodetachment from Aqueous Hydroxide. *J. Chem. Phys.* **2004**, *120*, 11712–11725.

(7) Sheu, W. S.; Rossky, P. J. *Chem. Phys. Lett.* **1993**, *202*, 186. Sheu, W. S.; Rossky, P. J. *Chem. Phys. Lett.* **1993**, *213*, 233. Sheu, W. S.; Rossky, P. J. Charge-Transfer-To-Solvent Spectra of an Aqueous Halide Revisited via Computer Simulation. *J. Am. Chem. Soc.* **1993**, *115*, 7729–7735. Bradforth, S. E.; Jungwirth, P. Excited States of Iodide Anions in Water: A Comparison of the Electronic Structure in Clusters and in Bulk Solution. *J. Phys. Chem. A* **2002**, *106*, 1286–1298.

(8) Borgis, D.; Staib, A. Quantum Adiabatic Umbrella Sampling: The Excited State Free Energy Surface of an Electron-Atom Pair in Solution. *J. Chem. Phys.* **1996**, *104*, 4776–4783. Staib, A.; Borgis, D. Reaction Pathways in The Photodetachment of an Electron From Aqueous Chloride: A Quantum Molecular Dynamics Study. *J. Chem. Phys.* **1996**, *104*, 9027–9039.

- (9) Elles, C. G.; Shkrob, I. A.; Crowell, R. A.; Arms, D. A.; Landahl, E. C. Transient X-ray Absorption Spectroscopy of Hydrated Halogen Atom. *J. Chem. Phys.* **2008**, *128*, 061102.
- (10) Sevilla, M. D.; Summerfeld, S.; Eliezer, I.; Rak, J.; Symons, M. C. R. Interaction of the Chlorine Atom with Water: ESR and Ab Initio MO Evidence for Three-Electron ($\sigma^2\sigma^{*1}$) Bonding. *J. Phys. Chem. A* **1997**, *101*, 2910–2915.
- (11) Roeselova, M.; Kaldor, U.; Jungwirth, P. Ultrafast Dynamics of Chlorine–Water and Bromine–Water Radical Complexes Following Electron Photodetachment in Their Anionic Precursors. *J. Phys. Chem. A* **2000**, *104*, 6523–6531. Roeselova, M.; Jacoby, G.; Kaldor, U.; Jungwirth, P. Relaxation of Chlorine Anions Solvated in Small Water Clusters upon Electron Photodetachment: The Three Lowest Potential Energy Surfaces of the Neutral Cl···H₂O Complex. *Chem. Phys. Lett.* **1998**, *293*, 309–316.
- (12) Li, J.; Li, Y.; Guo, H. Covalent Nature of X···H₂O (X = F, Cl, and Br) Interactions. *J. Chem. Phys.* **2013**, *138*, 141102.
- (13) Nagarajan, V.; Fessenden, R. W. Flash Photolysis of Transient Radicals. 1. X₂[−] with X = Cl, Br, I, and SCN. *J. Phys. Chem.* **1985**, *89*, 2330–2335. Lind, J.; Shen, X.; Eriksen, T. E.; Merenyi, G.; Eberson, L. One-Electron Reduction of N-Bromosuccinimide. Rapid Expulsion of a Bromine Atom. *J. Am. Chem. Soc.* **1991**, *113*, 4629–4633. Zehavi, D.; Rabani, J. Oxidation of Aqueous Bromide Ions by Hydroxyl Radicals. Pulse Radiolytic Investigation. *J. Phys. Chem.* **1972**, *76*, 312–319.
- (14) Hallett, J. P.; Welton, T. Room-Temperature Ionic Liquids: Solvents for Synthesis and Catalysis. 2. *Chem. Rev.* **2011**, *111*, 3508–3576. Welton, T. Room-Temperature Ionic Liquids. Solvents for Synthesis and Catalysis. *Chem. Rev.* **1999**, *99*, 2071–2083. Plechkova, N. V.; Seddon, K. R. Applications of Ionic Liquids in the Chemical Industry. *Chem. Soc. Rev.* **2008**, *37*, 123–150. Smiglak, M.; Metlen, A.; Rogers, R. D. The Second Evolution of Ionic Liquids: From Solvents and Separations to Advanced Materials: Energetic Examples from the Ionic Liquid Cookbook. Accounts. *Chem. Res.* **2007**, *40*, 1182–1192. Parvulescu, V. I.; Hardacre, C. Catalysis in Ionic Liquids. *Chem. Rev.* **2007**, *107*, 2615–2665. Binnemans, K. Lanthanides and Actinides in Ionic Liquids. *Chem. Rev.* **2007**, *107*, 2592–2614.
- (15) Wishart, J. F. *J. Phys. Chem. Lett.* **2010**, *1*, 3225–3231. Wishart, J. F.; Shkrob, I. A. In *Ionic Liquids: From Knowledge to Application*; Rogers, R. D., Plechkova, N. V., Seddon, K. R., Eds.; American Chemical Society: Washington, D.C., 2009; pp 119–134. Shkrob, I. A.; Wishart, J. F. Free Radical Chemistry in Room-Temperature Liquids. In *Handbook of Radical Chemistry and Biology*; Chatgilialoglu, C., Studer, A., Eds.; John Wiley & Sons: Chichester, U.K., 2012; pp 433–448.
- (16) Sun, X. Q.; Luo, H. M.; Dai, S. Ionic Liquids-Based Extraction: A Promising Strategy for the Advanced Nuclear Fuel Cycle. *Chem. Rev.* **2012**, *112*, 2100–2128. Wishart, J. F. Ionic Liquids and Ionizing Radiation: Reactivity of Highly Energetic Species. *J. Phys. Chem. Lett.* **2010**, *1*, 3225–3231.
- (17) Shkrob, I. A.; Wishart, J. F. Charge Trapping in Imidazolium Ionic Liquids. *J. Phys. Chem. B* **2009**, *113*, 5582–5592.
- (18) Shkrob, I. A.; Marin, T. W.; Chemerisov, S. D.; Wishart, J. F. Radiation Induced Redox Reactions and Fragmentation of Constituent Ions in Ionic Liquids. 1. Anions. *J. Phys. Chem. B* **2011**, *115*, 3872–3888.
- (19) Shkrob, I. A.; Marin, T. W.; Chemerisov, S. D.; Hatcher, J. L.; Wishart, J. F. Radiation Induced Redox Reactions and Fragmentation of Constituent Ions in Ionic Liquids. 2. Imidazolium Cations. *J. Phys. Chem. B* **2011**, *115*, 3889–3902.
- (20) Shkrob, I. A. Deprotonation and Oligomerization in Photo-, Radiolytically, and Electrochemically Induced Redox Reactions in Hydrophobic Alkylalkylimidazolium Ionic Liquids. *J. Phys. Chem. B* **2010**, *114*, 368–375.
- (21) Shkrob, I. A.; Chemerisov, S. D.; Wishart, J. F. The Initial Stages of Radiation Damage in Ionic Liquids and Ionic Liquid-Based Extraction Systems. *J. Phys. Chem. B* **2007**, *111*, 11786–11793.
- (22) Shkrob, I. A.; Marin, T. W.; Chemerisov, S. D.; Hatcher, J. L.; Wishart, J. F. Toward Radiation-Resistant Ionic Liquids. Radiation Stability of Sulfonyl Imide Anions. *J. Phys. Chem. B* **2012**, *116*, 9043–9055.
- (23) Shkrob, I. A.; Marin, T. W.; Chemerisov, S. D.; Wishart, J. F. Radiation and Radical Chemistry of NO₃[−], HNO₃, and Dialkylphosphoric Acids in Room-Temperature Ionic Liquids. *J. Phys. Chem. B* **2011**, *115*, 10927–10942.
- (24) Chandrasekhar, N.; Unterreiner, A.-N. Photochemical Processes in Ionic Liquids on Ultrafast Timescales. *Phys. Chem. Chem. Phys.* **2010**, *12*, 1698–1708.
- (25) Chandrasekhar, N.; Schalk, O.; Unterreiner, A.-N. Femtosecond UV Excitation in Imidazolium-Based Ionic Liquids. *J. Phys. Chem. B* **2008**, *112*, 15718–15724.
- (26) Brands, H.; Chandrasekhar, N.; Unterreiner, A.-N. Ultrafast Dynamics of Room Temperature Ionic Liquids after Ultraviolet Femtosecond Excitation. *J. Phys. Chem. B* **2007**, *111*, 4830–4836.
- (27) Katoh, R.; Yoshida, Y.; Katsumura, Y.; Takahashi, K. Electron Photodetachment from Iodide in Ionic Liquids through Charge-Transfer-to-Solvent Band Excitation. *J. Phys. Chem. B* **2007**, *111*, 4770–4774.
- (28) Wang, Z. P.; Zhang, L.; Chen, X. H.; Cukier, R. I.; Bu, Y. Excess Electron Solvation in an Imidazolium-Based Room-Temperature Ionic Liquid Revealed by Ab Initio Molecular Dynamics Simulations. *J. Phys. Chem. B* **2009**, *113*, 8222–8226. Wang, Z. P.; Zhang, L.; Chen, X. H.; Cukier, R. I.; Bu, Y. States and Migration of an Excess Electron in a Pyridinium-Based, Room-Temperature Ionic Liquid: an Ab Initio Molecular Dynamics Simulation Exploration. *Phys. Chem. Chem. Phys.* **2010**, *12*, 1854. See also Margulis, C. J.; Annapureddy, H. V. R.; De Biase, P. M.; Coker, D.; Kohanoff, J.; Del Popolo, M. G. Dry Excess Electrons in Room-Temperature Ionic Liquids. *J. Am. Chem. Soc.* **2011**, *133*, 20186.
- (29) Liu, J.; Wang, Z.; Zhang, M.; Cuckier, R. I.; Bu, Y. Excess Dielectron in an Ionic Liquid as a Dynamic Bipolaron. *Phys. Rev. Lett.* **2013**, *110*, 107602.
- (30) Shkrob, I. A.; Marin, T. W.; Wishart, J. F. *J. Phys. Chem. B* **2013**, in preparation.
- (31) Michalski, R.; Sikora, A.; Adamus, J.; Marcinek, A. Dihalide and Pseudothalide Radical Anions as Oxidizing Agents in Nonaqueous Solvents. *J. Phys. Chem. A* **2010**, *114*, 861–866.
- (32) Grodkowski, J.; Nyga, M.; Mirkowski, J. Formation of Br₂^{•−}, BrSCN^{•−} and (SCN)₂^{•−} Intermediates in the Ionic Liquid Methyltributylammonium Bis[(trifluoromethyl)sulfonyl]imide. Pulse Radiolysis Study. *Nukleonika* **2005**, *50* (Supplement 2), S35–S38.
- (33) Grodkowski, J.; Neta, P. Formation and Reaction of Br₂[•] Radicals in the Ionic Liquid Methyltributylammonium Bis-(trifluoromethylsulfonyl)imide and in Other Solvents. *J. Phys. Chem. A* **2002**, *106*, 11130–11134.
- (34) Becke, A. D. Density-Functional Exchange-Energy Approximation with Correct Asymptotic Behavior. *Phys. Rev. A* **1988**, *38*, 3098–3100. Lee, C.; Yang, W.; Parr, R. G. Development of the Colle-Salvetti Correlation-Energy Formula into a Functional of the Electron Density. *Phys. Rev. B* **1988**, *37*, 785–789.
- (35) Frisch, M. J.; Trucks, G. W.; Schlegel, H. B.; Scuseria, G. E.; Robb, M. A.; Cheeseman, J. G.; Montgomery, J. A., Jr.; Vreven, K. N.; Kudin, J. C.; Burant, J. C.; et al. *Gaussian 03*, revision C.02; Gaussian, Inc.: Wallingford CT, 2004.
- (36) Muto, H.; Kispert, L. D. An ESR Study at 77 K of the Bromine Atom and the >N–Br^{•−} σ* Radical in X-irradiated N-Bromosuccinimide Single Crystals. *J. Chem. Phys.* **1980**, *72*, 2300–2309.
- (37) Griscom, D. L. Electron Spin Resonance Observations Of Chlorine And Bromine Atoms Isolated at 22 K in X-irradiated Alkali Halide: Alkali Borate Glasses. *Solid State Commun.* **1972**, *11*, 899–902.
- (38) Preston, T. J.; Shaloski, M. A.; Crim, F. F. Probing the Photoisomerization of CHBr₃ and CHI₃ in Solution with Transient Vibrational and Electronic Spectroscopy. *J. Phys. Chem. A* **2013**, *117*, 2899–2907. Carrier, S. L.; Preston, T. J.; Dutta, M.; Crowther, A. C.; Crim, F. F. Ultrafast Observation of Isomerization and Complexation in the Photolysis of Bromoform in Solution. *J. Phys. Chem. A* **2010**, *114*, 1548–1555. George, L.; Kalume, A.; Esselman, B.; McMahon, R. J.; Reid, S. A. Pulsed Jet Discharge Matrix Isolation and Computational

Study of Bromine Atom Complexes: Br...BrXCH₂ (X = H, Cl, Br). *J. Phys. Chem. A* **2011**, *115*, 9820–9827.

(39) Shouote, L. C. T.; Neta, P. Bromine Atom Complexes with Bromoalkanes: Their Formation in the Pulse Radiolysis of Di-, Tri-, and Tetrabromomethane and Their Reactivity with Organic Reductants. *J. Phys. Chem.* **1990**, *94*, 2447–2453. Merenyi, G.; Lind, J. Reaction Mechanism of Hydrogen Abstraction by the Bromine Atom in Water. *J. Am. Chem. Soc.* **1994**, *116*, 7872–7876.

(40) Scaiano, J. C.; Barra, M.; Krzywinski, M.; Sinta, R.; Calabrese, G. Laser Flash Photolysis Determination of Absolute Rate Constants for Reactions of Bromine Atoms in Solution. *J. Am. Chem. Soc.* **1993**, *115*, 8340–8344. Khanna, R. K.; Armstrong, B.; Cui, H.; Tanko, J. M. Inverted Regioselectivities in the Reactions of Chlorine Atoms with Heteroarylmethanes. *J. Am. Chem. Soc.* **1992**, *114*, 6003–6006.

(41) Weldon, D.; Barra, M.; Sinta, R.; Scaiano, J. C. Dynamics of the Photochemical Debromination of Silicon-Substituted Vicinal Dibromides. *J. Org. Chem.* **1995**, *60*, 3921–3923.

(42) Lemal, D. M.; Lovald, R. A.; Kawano, K. I. Tetraaminoethylenes. The Question of Dissociation. *J. Am. Chem. Soc.* **1964**, *86*, 2518–2519. Chen, Y.-T.; Jordan, F. Reactivity of the Thiazolium C2 Ylide in Aprotic Solvents: Novel Experimental Evidence for Addition rather than Insertion Reactivity. *J. Org. Chem.* **1991**, *56*, 5029–5038. Alder, R. W.; Chaker, L.; Paolini, F. P. Bis(diethylamino)carbene and the Mechanism of Dimerisation for Simple Diaminocarbenes. *J. Chem. Soc., Chem. Commun.* **2004**, 2172–2173.